Aus dem NeuroCure Clinical Research Center
Exzellenzcluster NeuroCure
Campus Charité Mitte
der Medizinischen Fakultät Charité – Universitätsmedizin Berlin

DISSERTATION

Der Stellenwert der optischen Kohärenztomografie in der Diagnostik und Differentialdiagnostik von Erkrankungen des zentralen Nervensystems

zur Erlangung des akademischen Grades

Doctor medicinae (Dr. med.)

vorgelegt der Medizinischen Fakultät
Charité – Universitätsmedizin Berlin

von

Falko Andreas Kaufhold

aus Eberswalde-Finow

Datum der Promotion: 22.06.2014

Inhaltsverzeichnis

Abkürzungsverzeichnis

EDSS	Extended Disability Status Scale
GEE	Generalized estimation equation (verallgemeinerte Schätzgleichungen)
ICP	Intrakranieller Druck
IIH	Idiopathische intrakranielle Hypertension
MS	Multiple Sklerose
MSNON	MS-Patienten ohne eine vorangegangene Neuritis nervi optici
MSON	MS-Patienten mit eine vorangegangener Neuritis nervi optici
MRT	Magnetresonanztomographie
OCT	Optische Kohärenztomografie
ON	Neuritis nervi optici
ONHV	Optic Nerve Head Volume (Volumen des Sehnervenkopfes)
ONHH	Optic Nerve Head Height (maximale Höhe der Schwellung des Sehnervenkopfes)
PPMS	Primär progrediente Multiple Sklerose
RNFL	Retinale Nervenfaserschicht, welche alle Axone beinhaltet, die Informationen von den Ganglionzellen der Retina zum Gehirn transportieren
RRMS	Schubförmig remittierende Multiple Sklerose
SDOCT	Spectral domain OCT-Gerät
SPMS	Sekundär progrediente Multiple Sklerose
TMV	Totales Makulavolumen

1. Abstrakt (Deutsche Fassung)

Die optische Kohärenztomografie (OCT) ist ein neues, vielversprechendes Verfahren zur in vivo Untersuchung der Retina bezüglich der Degeneration von Axonen und Neuronen. In der Diagnostik der Multiplen Sklerose (MS) wird die Technik bereits zur Verlaufskontrolle bei Patienten mit und ohne Neuritis nervi optici (ON) angewendet.

Unser erstes Projekt, eine MS-Multicenterstudie, schloss 414 Patienten und 94 gesunde Kontrollpersonen ein. Die MS-Patienten zeigten dabei in 308 Fällen einen schubförmig-remittierenden (RRMS), in 65 Fällen einen sekundär-progredienten (SPMS) und in 41 Fällen einen chronisch-progredienten Krankheitsverlauf (PPMS). Unsere OCT-Daten konnten die von anderen Arbeitsgruppen gezeigte Verdünnung der Schicht retinaler Axone, welche sich zum Sehnerven bündeln (Retinal nerve fiber layer; RNFL), sowohl bei Patienten ohne ON ($p < 0,001$), als auch wesentlich stärker bei Patienten mit ON ($p < 0,001$) bestätigen. Die große Fallzahl an Patienten mit progressiven Verlaufsformen der MS erlaubte es uns erstmalig statistisch robust nachzuweisen, dass die RNFL-Dicke bei SPMS-Patienten ($p = 0,007$) wesentlich stärker abnimmt als bei RRMS-Patienten. Dies trifft auch für das totale Makulavolumen von SPMS-Patienten ($p = 0,039$) und von PPMS-Patienten ($p = 0,005$) im Vergleich zu RRMS-Patienten zu.

Die Susac-Studie untersuchte Patienten mit dem Susac-Syndrom, einer Differentialdiagnose der MS, mittels OCT. Wir konnten neun Patienten dieses seltenen Krankheitsbildes mit neun gesunden Kontrollpersonen und jeweils neun RRMS-Patienten mit bzw. ohne ON vergleichen. Die Susac-Patienten zeigten eine deutliche Abnahme der RNFL-Dicke im Vergleich zu gesunden Kontrollpersonen ($p < 0,001$), RRMS ohne ON ($p = 0,001$) und RRMS mit ON ($p = 0,019$). Im Gegensatz zur MS war die RNFL-Reduktion bei Susac-Patienten in charakteristischen Verteilungsmustern, vereinbar mit der vermuteten Pathogenese der Erkrankung durch retinale Arterienastverschlüsse, darstellbar.

In der IIH-Studie untersuchten wir 19 Patienten mit idiopathischer intrakranieller Hypertension (IIH) mittels OCT. Hierbei ging es speziell um die Etablierung eines neuen OCT-Markers zur Therapie und Verlaufskontrolle. Wir bestimmten neben der RNFL-Dicke zusätzlich das Volumen des Sehnerven (Optic nerve head volume; ONHV) und die maximale Höhe des Sehnerven. Das ONHV konnte die Schwellung des Sehnerven bei IIH-Patienten wesentlich besser darstellen als die Dicke der RNFL ($p < 0,001$). Weiterhin konnte eine Beziehung von ONHV und dem gemessenen Liquordruck

festgestellt werden (p = 0,004). Dieses Ergebnis deutet auf die Möglichkeit hin, zukünftig eventuell den Hirndruck mittels OCT bestimmen zu können. Zusammenfassend konnten wir mit unseren Studien vielversprechende Verwendungsmöglichkeiten der OCT für das Susac-Syndrom und IIH aufzeigen und die Datenlage zur MS weiter präzisieren und ausbauen.

2. Abstrakt (Englische Fassung)

Optical coherence tomography (OCT) is a fast and novel alternative for in vivo monitoring of retinal pathologies, especially axonal and neuronal degeneration. Nowadays OCT has already become a diagnostic tool to follow multiple sclerosis (MS) patients with (MSON) and without a history of optic neuritis (MSNON).

The first study, the MS-Multicenter study, included 414 patients and 94 healthy controls. Here, 308 MS patients had a relapsing remitting (RRMS), while 65 cases showed a secondary progressive (SPMS) and 41 patients presented with a primary progressive MS (PPMS). Using OCT we confirmed the previously described thinning of the retinal nerve fiber layer (RNFL) in MSNON patients ($p < 0.001$) as well as in a more severe way in patients with ON ($p < 0.001$). The large number of patients with progressive disease types allowed us to show for the first time in a statistical robust model that SPMS patients develop a more severe thinning of the RNFL than RRMS patients ($p = 0.007$). Moreover, this association was also observed in a decrease of the total macula volume of SPMS ($p = 0.039$) and PPMS patients ($p = 0.005$) in contrast to RRMS patients.

The Susac study investigated patients with Susac syndrome, a potential differential diagnosis of MS, using OCT. It compared nine patients with Susac syndrome with nine healthy controls and nine patients with RRMS with and without a previous ON. Patients with Susac syndrome showed a thinning of the RNFL in comparison to healthy controls ($p < 0.001$), RRMS-MSNON ($p = 0.001$) and RRMS-MSON ($p= 0.019$). In contrast to findings in MS patients, who presented predominantly with a thinning of the temporal quadrant of the RNFL, Susac patients exhibited more differentiated patterns of retinal damage consistent with the potential pathogenesis of retinal artery occlusions.

The IIH study investigated 19 patients with idiopathic intracranial hypertension (IIH) using OCT with the aim to establish a new parameter for follow-up and perhaps therapy control in IIH. Therefore, we measured optic nerve head volume (ONHV) and height

besides the thickness of the RNFL. ONHV indicated optic disc swelling more precise than RNFL thickness ($p < 0.001$). Additionally, an increased ONHV was associated with a higher intracranial pressure (ICP; $p = 0.004$), eventually proposing ONHV for monitoring ICP.
In summary, our studies suggest OCT as an additional diagnostic tool for Susac syndrome and IIH, and contribute to our knowledge on OCT in MS.

3. Einleitung

Die Multiple Sklerose (MS) ist eine chronische Autoimmunerkrankung des zentralen Nervensystems, welche über fokal-demyelinisierende Prozesse sowohl axonalen als auch neuronalen Schaden verursacht und zu einer Vielzahl neurologischer Manifestationen führen kann. Die Erkrankung kann sowohl schubförmig remittierend (RRMS), sekundär progredient (SPMS), als auch chronisch progredient (PPMS) verlaufen und manifestiert sich in 25 – 50% der Fälle mit dem Erstsymptom einer Neuritis nervi optici (ON) (1,2). Im Rahmen dieses Entzündungsprozesses wird besonders die retinale Nervenfaserschicht (RNFL), welche alle Axone umfasst, die visuelle Informationen vom Auge zum Gehirn transportieren, durch inflammatorische Prozesse geschädigt. Die optische Kohärenztomografie (OCT) ist ein Verfahren aus der Ophthalmologie und bietet dem Untersucher die Möglichkeit, die Netzhautschichten inklusive der RNFL schnell und detailliert in vivo darzustellen und damit die axonale Degeneration direkt zu beurteilen. Aktuelle Studien zeigen sowohl eine Abnahme der Dicke der RNFL bei MS Patienten nach einer ON (MSON) (3,4), als auch solchen ohne eine ON im Krankheitsverlauf (MSNON), wobei in diesem Fall eine kontinuierliche neuroaxonale Degeneration im Gegensatz zu subklinisch verlaufenden ONs diskutiert wird (5). Die Datenlage bezüglich RNFL-Veränderungen in den unterschiedlichen MS-Subtypen mit bzw. ohne ON ist teilweise widersprüchlich, daher versuchten wir in einer Multicenterstudie mit einer großen Fallzahl dieses Thema detaillierter zu untersuchen.
Die vielversprechenden Ergebnisse in der MS-Forschung machen die OCT auch für die Anwendung bei weiteren neurologischen Krankheitsbildern, welche ähnlich der MS pathologische Veränderungen der Retinastrukturen zur Folge haben können, interessant. Im Rahmen dieser Hypothese untersuchten wir zum Einen Patienten mit dem Susac-Syndrom, einer seltenen, vermutlich autoimmunen Erkrankung, die durch eine Symptomtrias aus Enzephalopathie, sensorineuronalem Gehörverlust und

Gesichtsfelddefekten charakterisiert ist, wobei die visuellen Symptome vermutlich durch Verschlüsse retinaler Arterienäste verursacht werden. Ähnlich der MS manifestiert sich die Erkrankung vorwiegend bei Frauen zwischen 20 und 40 Jahren (6). Während Hörverlust und Sehbeeinträchtigung nicht zwingend zum Krankheitsbeginn dominieren, äußert sich die Enzephalopathie meistens schon zu Krankheitsbeginn in starken Kopfschmerzen, sowie fokal neurologischen und neuropsychiatrischen Defiziten. Die Diagnose lässt sich unter anderem mittels Magnetresonanztomographie (MRT) stellen. Hier zeigen sich pathognomonische Läsionen im Corpus callosum (7). Wird nicht die komplette Symptomtrias beachtet, kann es aufgrund ähnlicher bildmorphologischer Befunde im zerebralen MRT und der visuellen Symptome zur Fehldiagnose MS kommen. Dadurch besteht die Möglichkeit, dass die Patienten eine nicht indizierte immunmodulatorische Therapie anstatt einer immunsuppressiven Therapie erhalten, welche für das Susac-Syndrom in der Regel gefordert wird (8). Zur Vermeidung dieses Szenarios besteht ein großer Bedarf an differential-diagnostischen Alternativen, um den Patienten eine adäquate Therapie auf Basis einer schnellen Diagnose, zu ermöglichen.

Zum Zweiten untersuchten wir Patienten mit idiopathischer intrakranieller Hypertension (IIH), einem klinischen Syndrom verursacht durch erhöhten intrakraniellen Druck (ICP) ohne bildmorphologisches Korrelat im MRT. Diese Erkrankung betrifft vor allem junge, gebärfähige und adipöse Frauen, welche vorwiegend über dauerhafte Kopfschmerzen, visuelle Symptome, Tinnitus und Schwindel klagen (9). Die schwerwiegendste Komplikation dieses Syndroms ist die durch den erhöhten intrakraniellen Druck verursachte Stauungspapille mit der Langzeitfolge einer Erblindung bei bis zu 10 Prozent der Patienten (10). Erste querschnittliche OCT-Studien bei IIH-Patienten zeigten eine signifikante Verdickung der RNFL bei neu diagnostizierten Patienten und legten die Verwendung der RNFL-Messung mittels OCT als diagnostischen Parameter dieser Erkrankung nahe (11,12). Da die RNFL-Messung jedoch nur den Grenzbereich des Schwellungsprozesses einer Stauungspapille erfasst, konzentrierten wir uns auf die Bestimmung des Volumens des Sehnerven, um etwaige morphologische Veränderungen genauer beurteilen zu können.

Zusammenfassend war somit das Ziel unserer Studien, die mögliche Verwendung der OCT im Rahmen der Diagnostik und Verlaufskontrolle der MS weiter zu evaluieren und vor allem die differentialdiagnostischen Möglichkeiten der OCT bei weiteren neurologischen Erkrankungen wie dem Susac-Syndrom und IIH zu bewerten.

4. Patienten und Methodik

4.1. Patienten

Die MS Multicenter-Studie erfasste 414 MS-Patienten und 94 gesunde Kontrollpersonen, rekrutiert an der Heinrich-Heine-Universität Düsseldorf, an der Universitätsklinik Hamburg-Eppendorf und an der Charité in Berlin. MS-Patienten wurden eingeschlossen, wenn sie nach den überarbeiteten McDonald-Kriterien von 2005 diagnostiziert wurden (13). Die Unterteilung der MS-Subtypen wurde nach den Lublin-Kriterien vorgenommen (14). Augen mit ON wurden in die Analyse eingeschlossen, wenn sie entweder klinisch dokumentiert waren, eine pathologische Latenzzeit von mehr als 115 ms in der Untersuchung von visuell evozierten Potentialen vorlag oder der Patient eine passende Anamnese aufwies. Das Geschlecht der Gruppe gesunder Kontrollen unterschied sich nicht signifikant von den RRMS-Patienten ($p = 0,452$) und SPMS-Patienten ($p = 0,186$), während unter PPMS-Patienten ein deutlich größerer Anteil Männer als bei den Kontrollen auftrat ($p = 0,010$). Weiterhin war das Alter der gesunden Kontrollpersonen im Vergleich zu allen MS-Subtypen geringer ($p < 0,001$), auch RRMS-Patienten waren jünger als SPMS- und PPMS-Patienten ($p < 0,001$). Die Krankheitsdauer der RRMS- und PPMS-Patienten war deutlich kürzer als die der SPMS-Patienten ($p < 0,001$). Folglich wurden alle statistischen Analysen für Alter, Geschlecht und Krankheitsdauer korrigiert (15).

Im Rahmen der Susac-Studie wurden neun Patienten mit Susac-Syndrom (Mittelwert ± Standardabweichung für Alter: 33 ± 11 Lebensjahre [min. 20 – max. 47]) mit jeweils neun gesunden Kontrollpersonen, Patienten mit RRMS ohne vorherige ON und Patienten mit RRMS und vorangegangen bilateralen ON verglichen. Geschlechtsspezifisch und altersspezifisch gab es keine Unterschiede zwischen den Studiengruppen. In der Susac-Patientenkohorte wurden sechs Frauen und drei Männer eingeschlossen. Dies entspricht der Geschlechtsverteilung, welche in der Literatur berichtet wird (7). Auch die Krankheitsdauer der RRMS-Patienten unterschied sich nicht signifikant von jener der Susac-Patienten ($p = 0,062$). Keiner der untersuchten Susac- bzw. MS-Patienten hatte zum Zeitpunkt der OCT-Messung eine klinisch aktive Krankheitsphase (16).

In der IIH-Studie wurden 19 Patienten (Mittelwert ± Standardabweichung für Alter: 38,0 ± 13,8; für BMI: 33,6 ± 7,4) mit idiopathischer intrakranieller Hypertension (IIH), diagnostiziert nach den modifizierten Dandy-Kriterien (17), und 19 adipöse

Kontrollpersonen (Mittelwert ± Standardabweichung für Alter 37,6 ± 12,9; für BMI 33,8 ± 7,3) mittels OCT untersucht. Die beiden Gruppen unterschieden sich nicht in Bezug auf Alter, Geschlecht und Body-Mass-Index (18).

4.2. Optische Kohärenztomographie

Die optische Kohärenztomographie stellt ein schnelles, nicht invasives und nebenwirkungsarmes Verfahren zur Untersuchung der Netzhaut dar. Während einer kurzen Untersuchungszeit von zehn Minuten pro Auge tastet ein Laser die Retina ab und erzeugt ein „histologisches“ Querschnittsbild. Das Grundprinzip beruht auf der Interferometrie. Hierbei wird Licht einer geringen Kohärenzlänge in das Auge geworfen und von den verschiedenen Schichten der Netzhaut reflektiert, wieder aufgefangen und mit der Weglänge des Lichtes in einem Referenzarm verrechnet (19).

Für unsere Studien verwendeten wir 2 unterschiedliche OCT-Geräte, zum Einen das Stratus 3000 OCT (Carl Zeiss Meditec, California, USA) für die Susac-Studie und zum Zweiten das weiterentwickelte Heidelberg Spectralis SDOCT (Heidelberg Engineering, Germany) für die MS- und die IIH-Studie. Mithilfe dieser Geräte wurden studienspezifisch die Dicke der RNFL, das totale Makulavolumen (TMV), das Volumen des Sehnerven (ONHV) und die maximale Höhe des Sehnerven (ONHH) bestimmt. Beide Geräte unterscheiden sich bezüglich Schnelligkeit und Auflösung der Bilder, weshalb die Messerergebnisse der Studien untereinander nicht miteinander verglichen werden können (20).

Die RNFL wird durch einen peripapillären Ringscan in einem Abstand von 3,4 mm um den Sehnerv erfasst. Hierzu wurde das im Gerät integrierte Standardprotokoll verwendet, welches über einen automatischen Segmentierungsalgorithmus die Dicke der RNFL bestimmt. Weiterhin wurde für die Susac-Studie das TMV mittels des im Stratus-OCT integrierten Standardmessprotokolls bestimmt. Die Volumenscans der Makula und des Sehnerven wurden für die IIH-Studie und die MS-Multicenterstudie mit modifizierten Messprotokollen erfasst. Zur detaillierteren Quantifizierung der Schwellung des Sehnerven wurde ein vollautomatischer Auswertungsalgorithmus entwickelt. Vereinfacht wurde hierbei eine virtuelle Verlängerung des retinalen Pigmentepithels durch den Sehnerv für jeden B-Scan generiert, welche als untere Grenze des Volumens diente. Die obere Grenze wurde durch die Membrana limitans interna festgesetzt. Daraus wurden dann ONHV und ONHH berechnet. Eine detaillierte Beschreibung des

Algorithmus ist durch Kadas et al. in Bildverarbeitung für die Medizin 2012 nachzulesen (21).

4.3. Statistik

Für die MS-Multicenterstudie und die IIH-Studie wurden die Unterschiede zwischen den Gruppen mithilfe des Mann-Whitney U Test für Alter, EDSS bzw. BMI berechnet. Geschlechtsunterschiede wurden für die MS-Studie mittels Chi-Quadrat-Test untersucht. In der Susac-Studie berechneten wir die Gruppenunterschiede für Alter und Krankheitsdauer mithilfe der Friedman Analyse für gematchte Paare.

In allen drei Studien wurden verallgemeinerte Schätzgleichungen (generalized estimated equation; GEE) benutzt, um die Unterschiede zwischen den Augen der Patientengruppen zu berechnen. Diese Modelle erlauben die separate Auswertung der beiden Augen einer Person, berücksichtigen hierbei jedoch auch die stärkere Korrelation beider Augen einer Person miteinander. Bestanden Unterschiede in Bezug auf Alter, Geschlecht oder Krankheitsdauer zwischen den zu untersuchenden Gruppen, so wurden die verallgemeinerten Schätzgleichungen für diese Unterschiede korrigiert.

Für die IIH-Studie wollten wir weiterhin den Zusammenhang zwischen intrakraniellem Druck (ICP) und ONHV mittels GEE untersuchen. Da die Hirndrücke unserer Patienten jedoch nicht immer zeitnah zur OCT-Messung erfasst werden konnten, schlossen wir nur Patienten mit einer ICP-Messung innerhalb der letzten zwei Jahre ein. Weiterhin multiplizierten wir die ONHV-Ergebnisse mit einem Faktor, der Messwerte mit einer aktuelleren ICP-Messung stärker gewichtete, als jene mit einem großen Zeitfenster zwischen OCT und ICP-Messung.

Alle statistischen Analysen wurden entweder mit SPSS 19 bzw. 20 oder mit R durchgeführt. Bei allen Berechnungen wurde statistische Signifikanz bei einem p-Wert $< 0,05$ definiert.

5. Ergebnisse

5.1. MS-Multicenterstudie

In der MS-Multicenterstudie konnten insgesamt 754 Augen von 414 MS-Patienten und 183 Augen von 94 gesunden Kontrollpersonen in die statistische Analyse eingeschlossen werden. 79 Augen mussten entweder aufgrund schlechter Qualität der OCT-Scans oder einer unvollständigen bzw. widersprüchlichen Dokumentation des

Krankheitsverlaufs in Bezug auf eine vorrangegangene ON ausgeschlossen werden. Die MS-Patienten untergliederten sich in 308 RRMS-Patienten mit insgesamt 156 MSON-Augen, 65 SPMS-Patienten mit 27 MSON-Augen und 41 PPMS-Patienten mit ausschließlich MSNON-Augen.

MSNON zeigten eine geringere RNFL als gesunde Kontrollpersonen ($p < 0,001$). Dies traf auch für die einzelnen MS-Subtypen zu (RRMS: $p < 0,001$; SPMS: $p < 0,001$; PPMS: $p < 0,001$). Weiterhin konnte eine Reduktion des TMV von MSNON, sowie der einzelnen MS-Subtypen im Vergleich zu gesunden Kontrollen festgestellt werden (MSNON: $p < 0,001$; RRMS: $p < 0,001$; SPMS: $p < 0,001$; PPMS: $p < 0,001$). Die RNFL der gesamten MSON-Kohorte (Mittelwert ± Standardabweichung: 77,88 ± 14,61 µm; $p < 0,001$), sowie auch separat für RRMS- und SPMS-Patienten ($p < 0,001$; $p = 0,001$), war reduziert im Vergleich zu MSNON-Patienten (Mittelwert ± Standardabweichung: 90,15 ± 12,27 µm). Zusätzlich zeigte sich die gleiche Tendenz auch für den Vergleich der TMV-Daten zwischen MSON und MSNON ($p < 0,001$), sowie spezifisch für RRMS ($p < 0,001$) und SPMS ($p = 0,012$).

In einer detaillierteren Analyse der MSNON-Patienten konnte festgestellt werden, dass die Abnahme der RNFL bei progressiven MS-Verlaufsformen deutlich stärker war, als bei der RRMS. Eine Signifikanz ergab sich jedoch nur für den Vergleich zwischen RRMS und SPMS ($p = 0,007$). Die TMV-Daten zeigten die gleiche Tendenz (RRMS versus SPMS: $p = 0,039$) und zusätzlich noch einen Unterschied zwischen RRMS und PPMS ($p = 0,005$). Auch eine Assoziation von RNFL-Dicke und TMV mit der Krankheitsdauer konnte in der MSNON-Kohorte nachgewiesen werden ($p < 0,001$). Diese zeigte sich nicht bei MSON-Patienten. Hypothetisch untersuchten wir die jährliche RNFL-Abnahme der MSNON-Patienten basierend auf der Krankheitsdauer im Vergleich zu gesunden Kontrollen. Hier zeigte sich der stärkste Effekt bei RRMS-Patienten (-0,495 µm pro Jahr), gefolgt von SPMS-Patienten (-0,464 µm pro Jahr), während die jährliche Abnahme bei PPMS-Patienten wesentlich geringer ausfiel (-0,105 µm pro Jahr) (15).

5.2. Susac-Studie

Für die Susac-Studie konnten alle 18 Augen der neun Susac-Patienten eingeschlossen werden. Ein dokumentierter Hörverlust im Krankheitsverlauf lag bei allen Patienten vor. Jeweils acht von neun Patienten zeigten visuelle Symptome und solche einer Enzephalopathie in der Anamnese.

Sieben der acht Patienten mit visuellen Symptomen zeigten verglichen mit der normativen Datenbank des Stratus-OCT entweder eine Verringerung der RNFL oder des TMV. Zusätzlich zeigte auch der Patient ohne dokumentierte visuelle Symptome im Krankheitsverlauf eine starke Verdünnung der RNFL im superioren Quadranten des rechten Auges im Vergleich zur normativen Datenbank. Weiterhin ist anzumerken, dass die Reduktion von RNFL und TMV nicht das gesamte vermessene Areal der Netzhaut gleichmäßig betraf, sondern sich bei jedem einzelnen Patienten in bestimmten, eingrenzbaren Quadranten der Retina manifestierte. Anders, als die bei MS-Patienten nachgewiesene typische Verdünnung des temporalen Quadranten der RNFL, zeigte sich bei Susac-Patienten ein „buntes“ Verteilungsmuster der RNFL-Reduktion mit Betonung der superioren und inferioren Quadranten der RNFL, passend zum Verlauf der Arterien der Retina.

Susac-Patienten zeigten eine dünnere RNFL sowohl im Vergleich zu gesunden Kontrollpersonen ($p < 0,001$), als auch zu RRMS Patienten ohne vorherige ON ($p = 0,001$) und zu RRMS mit vorangegangener ON ($p = 0,019$). Das TMV war nur im Vergleich zu gesunden Kontrollpersonen ($p = 0,001$) und zu RRMS-Patienten ohne ON ($p = 0,001$) reduziert (16).

5.3. IIH-Studie

Wir konnten insgesamt 37 Augen von 19 IIH-Patienten und 38 Augen von 19 Kontrollpersonen miteinander vergleichen. Aufgrund von epiretinalen Membranen musste ein Auge einer Patientin aus der Analyse ausgeschlossen werden. Die Patienten hatten eine durchschnittliche Krankheitsdauer von 40 Monaten (Min. 0 – Max. 115). Der zuletzt gemessene ICP betrug durchschnittlich 28,6 cmH_2O. Weiterhin wurden 13 der 19 Patienten pharmakologisch mit Azetazolamid, Topiramat oder Furosemid behandelt.

Im Rahmen der statischen Auswertung ergab sich kein Unterschied in RNFL-Dicke und TMV zwischen IIH-Patienten und den Kontrollprobanden (RNFL-Dicke: $p = 0,942$; TMV: $p = 0,141$). Der neu eingeführte Parameter ONHV war doppelt so hoch bei IIH-Patienten (Mittelwert ± Standardabweichung: 2,30 ± 1,25 mm^3) im Vergleich zu den Kontrollen (Mittelwert ± Standardabweichung: 1,08 ± 0,49 mm^3; $p < 0,001$). Zusätzlich lagen in Bezug auf das ONHV 18 Augen von 11 IIH-Patienten über der 95% Perzentile der Kontrollgruppe, während es für die RNFL-Dicke nur 7 Augen von 4 Patienten waren.

ONHH zeigte jedoch keinen Unterschied zwischen Kontrollen und Patienten (p = 0,099).
Eine weitere Unterteilung der Patientengruppe in medikamentös behandelte und unbehandelte Patienten zeigte ein signifikant erhöhtes ONHV bei Patienten die zum Untersuchungszeitpunkt unbehandelt waren (p < 0,001). Weiterhin konnte eine postitive Korrelation von ONHV und dem aktuell gemessenen Liquordruck festgestellt werden (p = 0.004) (18).

6. Diskussion

Viele neurologische Erkrankungen verursachen direkt Schäden am visuellen System. Die OCT bietet uns eine schnelle, nicht invasive und für den Patienten relativ angenehme Methode zur Beurteilung des Augenhintergrundes, speziell der Retina und ihrer einzelnen Schichten. Auf dem heutigen Stand der Forschung wird vor allem die RNFL-Dicke als aussagekräftiger Marker für neuro-axonalen Schaden im anterioren visuellen System diskutiert. Im Rahmen der hier vorgestellten Studien wurde diese Erkenntnis für die MS bestätigt und für weitere neurologische Krankheitsbilder untersucht.
Die Ergebnisse der MS-Multicenterstudie bestätigten größtenteils die Ergebnisse vorangegangener Studien in einer jedoch deutlich größeren Patientenkohorte und mit dem weiterentwickelten SDOCT. Wir konnten eine RNFL-Reduktion sowohl in MSON-, als auch MSNON-Augen im Vergleich zu gesunden Kontrollpersonen bestätigen, wobei MSON wesentlich stärker betroffen waren als MSNON. Die sehr große Fallzahl unserer Studie (414 MS-Patienten und 94 Kontrollen) verleiht diesen Ergebnissen zusätzliche Aussagekraft und birgt noch einen weiteren Vorteil. Im Gegensatz zu bereits publizierten Arbeiten auf diesem Gebiet konnten wir eine wesentlich größere Anzahl von Patienten mit progressiven Verlaufsformen untersuchen (65 SPMS; 41 PPMS). Wir konnten sowohl eine Reduktion der RNFL als auch des TMV bei SPMS-Patienten im Vergleich zu RRMS-Patienten finden. Dieser Befund steht im Gegensatz zu früheren Arbeiten (22,23), kann aufgrund der wesentlich höheren Fallzahl aber als statistisch robuster angesehen werden. Weiterhin zeigte sich auch eine Reduktion des TMV bei PPMS-Patienten im Vergleich zu RRMS-Patienten. Hieraus lässt sich schlussfolgern, dass die Netzhaut bei progressiven Verlaufsformen der MS wesentlich stärker betroffen

ist, als bei schubförmig remittierenden. Ein weiterer Vorteil unserer Studie ist die Verwendung des weiterentwickelten SDOCT. Diese weitentwickelte Technologie ermöglicht es zum Beispiel mithilfe der Eye-Tracker-Funktion eventuelle Messfehler durch Augenbewegungen des Patienten auszuschalten. Diese Möglichkeit besteht bei den für die meisten bereits publizierten Studien verwendeten Stratus-OCT Geräten nicht. Somit ergibt sich eine deutlich höhere Reliabilität der SDOCT-Aufnahmen auch aufgrund einer höheren Auflösung der SDOCT-Geräte, welche die Aussagekraft unserer Studie untermauert. Zusätzlich konnten wir eine weitaus stärkere jährliche Abnahme der RNFL-Dicke bei SPMS und RRMS-Patienten ohne ON in der Vorgeschichte im Vergleich zu PPMS-Patienten berechnen. Dieses Ergebnis ist von großem Interesse in Bezug auf die mögliche Verwendung der OCT als longitudinalem Marker für die MS und passt zu bereits publizierten Daten (22). Allerdings darf dieser Befund nicht überbewertet werden, da die Berechnung allein auf querschnittlichen Daten beruht.

In der Susac-Studie konnten wir nachweisen, dass pathologische Veränderungen der Retina im Rahmen dieses Krankheitsbildes mittels OCT darstellbar sind. Acht unserer neun untersuchten Patienten zeigten entweder eine Reduktion der RNFL oder des TMV. Wichtig in diesem Zusammenhang ist auch die Tatsache, dass diese Verringerung bei allen Patienten in bestimmten Quadranten der Retina gebündelt vorkam. Dieses Ergebnis passt sehr gut zu einem bereits publizierten Fall einer 23-jährigen Susac-Patientin mit charakteristischen, quadrantenspezifischen Abnahmen von RNFL-Dicke und Makulasektoren (24). Damit lässt sich die vermutete Pathogenese des Susac-Syndroms, wobei retinale Arterienastverschlüsse für die visuellen Symptome der Patienten verantwortlich sind, gut erklären. Folglich werden nur bestimmte, klar definierte Bereiche der Netzhaut betroffen in denen es aufgrund der Minderperfusion zu einem Verlust an Nervenfasern und damit auch an visueller Funktion kommt. Interessant wäre in diesem Zusammenhang auch die Frage, ob durch die Minderperfusion eine gleichmäßige Verdünnung aller Netzhautschichten entsteht, wie es zu erwarten wäre, oder ob einige Schichten stärker betroffen sind. Diese Fragestellung war mithilfe des für die Studie verwendeten Stratus-OCT leider nicht zu beantworten, da aufgrund der Technologie eine Differenzierung zwischen den einzelnen Retinaschichten im Vergleich zum neueren SDOCT nur begrenzt möglich ist und sollte daher in weiterführenden Studien beantwortet werden.

Sowohl RNFL-Dicke als auch TMV waren deutlich verringert bei Susac-Patienten im Vergleich zu gesunden Kontrollen und RRMS ohne ON. Die RNFL-Dicke zeigte weiterhin einen signifikanten Unterschied zu RRMS Patienten mit ON. Diese Ergebnisse zeigen, dass sich die OCT-Befunde von Susac-Patienten deutlich von denen von gesunden Kontrollpersonen und MS-Patienten unterscheiden. Somit legen sie eine mögliche Verwendung der OCT zur Differenzierung zwischen Susac und MS nahe, wenn zum Beispiel MRT-Ergebnisse nicht eindeutig sind. Die Tatsache, dass wir außerdem bei einem Patienten, der keine dokumentierte visuelle Symptomatik aufwies, trotzdem eine pathologische Veränderung des superioren Quadranten der RNFL des rechten Auges nachweisen konnten, unterstützt die Vermutung, dass die OCT eventuell charakteristische Veränderungen der Retina darstellen könnte, bevor diese sich klinisch manifestieren, und unterstreicht die zuvor genannte Verwendungsmöglichkeit.

In diesem Zusammenhang muss die tatsächliche Aussagekraft der OCT zur Differenzierung zwischen Susac und MS jedoch aufgrund einiger Limitationen unserer Studie kritisch betrachtet werden. Zum Einen ist die Fallzahl mit neun Patienten für die Seltenheit des Syndroms mit nur knapp über 200 beschriebenen Fällen zwar sehr hoch (7), jedoch nicht hoch genug, um den Ergebnissen letzte Nachhaltigkeit zu geben. Weiterhin wissen wir nicht, in welchem zeitlichen Abstand Pathologien der Retina und klinische Symptome auftreten. Damit ist die prognostische Bedeutung der OCT nicht genauer zu evaluieren. Fest steht, dass eine frühzeitig immunsuppressive Therapie die Prognose der Erkrankung deutlich verbessert (8) und der Mangel an differentialdiagnostischen Möglichkeiten eine zusätzliche Anwendung der bereits gut verfügbaren Stratus-OCT-Technologie den Patienten eher helfen würde, als ihnen zu schaden.

Das Krankheitsbild der idiopathischen intrakraniellen Hypertension betreffend konnte gezeigt werden, dass im Gegensatz zur bestehenden Studienlage die RNFL-Dicke als prognostischer Marker an Aussagekraft verliert. Die Schwellung des Sehnerven im Rahmen einer Stauungspapille wird durch die RNFL-Messung nur teilweise erfasst, da der Teil der Netzhaut, der bei der Messung untersucht wird, nur den Rand des Schwellungsprozesses darstellt. Mithilfe des neu etablierten ONHV konnten wir eine signifikante Differenz von durchschnittlich 1,22 mm^3 zwischen den IIH-Patienten und den Kontrollpersonen nachweisen ($p < 0,001$). Weiterhin identifizierte das ONHV-Messung deutlich mehr Patienten mit Schwellungen über der 95% Perzentile der Kontrollgruppe als die RNFL-Messung. Somit stellt das ONHV einen weitaus

vielversprechenderen Marker für diese Erkrankung dar, als die RNFL-Dicke. Zusätzlich zeigte unsere Studie, dass medikamentös unbehandelte Patienten eine wesentlich stärkere Schwellung aufwiesen, als medikamentös eingestellte Patienten. Dies zeigt, dass eine medikamentöse Therapie der Erkrankung ratsam erscheint, obwohl der Beweis durch klinische Studien offen bleibt (10). Weiterhin offeriert dieser Befund die Möglichkeit, die OCT eventuell als Verfahren zur Therapie- und Verlaufskontrolle der IIH zu verwenden. Unterstützt wird diese Möglichkeit von der im Rahmen der Studie nachgewiesenen positiven Korrelation zwischen ICP und ONHV, welche aufgrund der teilweise nicht aktuellen ICP-Werte nicht überbewertet werden darf, aber immerhin eine deutliche Tendenz für die mögliche Nutzbarkeit der OCT bei Krankheitsbildern mit erhöhtem ICP zeigt.

Neben der medikamentösen Therapie sollten IIH-Patienten vor allem eine Gewichtsreduktion anstreben (25). Weiterhin wird in Deutschland die Therapiekontrolle häufig mittels Lumbalpunktion durchgeführt. Der therapeutische Nutzen der Lumbalpunktion bei Patienten mit erhöhtem ICP ist unbestritten, allerdings ist die Lumbalpunktion einzig und allein zur Verlaufskontrolle bei IIH-Patienten, welche im Rahmen ihrer Krankengeschichte sehr häufig punktiert werden, angesichts einer schnellen und nebenwirkungsarmen Alternative durchaus zu diskutieren. Um diese Möglichkeit weiter in Betracht zu ziehen, müssen vor allem longitudinale Daten dieser Patientengruppe erhoben werden, um das ONHV weiter zu evaluieren und eventuell zu etablieren.

Zusammenfassend zeigten unsere Studien erstmals robuste Ergebnisse in Bezug auf die unterschiedliche Entwicklung der RNFL und des TMV progressiver MS-Krankheitsverläufe und konnten die bereits publizierten Ergebnisse bei MSON und MSNON mithilfe einer großen Fallzahl untersuchter Patienten untermauern. Weiterhin konnten wir die OCT als Alternative bei der Differentialdiagnostik zwischen Susac-Syndroms und MS vorstellen, wobei wir deutliche Unterschiede in Bezug auf RNFL und TMV zwischen Susac-Syndrom und MS nachweisen konnten. Letztlich wurde durch die IIH-Studie erstmals der Sehnerv von Patienten mit erhöhtem Hirndruck quantifiziert. Das ONHV stellt eine neue vielversprechende Alternative in der Therapie- und Verlaufskontrolle der IIH dar.

7. Literaturverzeichnis

1. Compston A, Coles A. Multiple sclerosis. Lancet. 2008. 25;372:1502–17.

2. Frohman E, Costello F, Zivadinov R, et al. Optical coherence tomography in multiple sclerosis. Lancet Neurol. 2006;5:853–63.

3. Trip SA, Schlottmann PG, Jones SJ, et al. Retinal nerve fiber layer axonal loss and visual dysfunction in optic neuritis. Ann Neurol. 2005;58:383–91.

4. Siger M, Dzięgielewski K, Jasek L, et al. Optical coherence tomography in multiple sclerosis. J Neurol. 2008;255:1555–60.

5. Petzold A, De Boer JF, Schippling S, et al. Optical coherence tomography in multiple sclerosis: a systematic review and meta-analysis. Lancet Neurol. 2010;9:921–32.

6. Susac JO, Egan RA, Rennebohm RM, Lubow M. Susac's syndrome: 1975–2005 microangiopathy/autoimmune endotheliopathy. J Neurol Sci. 2007;257:270–2.

7. Rennebohm R, Susac JO, Egan RA, Daroff RB. Susac's Syndrome — Update. J Neurol Sci. 2010;299:86–91.

8. Rennebohm RM, Susac JO. Treatment of Susac's syndrome. J Neurol Sci. 15. Juni 2007;257:215–20.

9. Kesler A, Hadayer A, Goldhammer Y, Almog Y, Korczyn AD. Idiopathic intracranial hypertension Risk of recurrences. Neurology. 2004;63:1737–9.

10. Ball AK, Clarke CE. Idiopathic intracranial hypertension. Lancet Neurol. 2006;5:433–42.

11. Skau M, Milea D, Sander B, Wegener M, Jensen R. OCT for optic disc evaluation in idiopathic intracranial hypertension. Graefes Arch Clin Exp Ophthalmol. 2011;249:723–30.

12. Skau M, Sander B, Milea D, Jensen R. Disease activity in idiopathic intracranial hypertension: a 3-month follow-up study. J Neurol. 2011;258:277–83.

13. Polman CH, Reingold SC, Edan G, et al. Diagnostic criteria for multiple sclerosis: 2005 revisions to the “McDonald Criteria”. Ann Neurol. 2005;58:840–6.

14. Lublin FD, Reingold SC. Defining the clinical course of multiple sclerosis: results of an international survey. National Multiple Sclerosis Society (USA) Advisory Committee on Clinical Trials of New Agents in Multiple Sclerosis. Neurology. 1996;46:907–11.

15. Oberwahrenbrock T, Schippling S, Ringelstein M, et al. Retinal Damage in Multiple Sclerosis Disease Subtypes Measured by High-Resolution Optical Coherence Tomography. Multiple Sclerosis International. 2012;2012:1–10.

16. Brandt AU, Zimmermann H, Kaufhold F, et al. Patterns of Retinal Damage Facilitate Differential Diagnosis between Susac Syndrome and MS. PLoS ONE. 2012;7:e38741.

17. Smith JL. Whence pseudotumor cerebri? J Clin Neuroophthalmol. 1985;5:55–6.

18. Kaufhold F, Kadas EM, Schmidt C, et al. Optic Nerve Head Quantification in Idiopathic Intracranial Hypertension by Spectral Domain OCT. PLoS ONE. 2012;7:e36965.

19. Huang D, Swanson EA, Lin CP, et al. Optical coherence tomography. Science. 1991;254:1178–81.

20. Knight OJ, Chang RT, Feuer WJ, Budenz DL. Comparison of Retinal Nerve Fiber Layer Measurements Using Time Domain and Spectral Domain Optical Coherent Tomography. Ophthalmology. 2009;116:1271–7.

21. Kadas EM, Kaufhold F, Schulz C, Paul F, Polthier K, Brandt AU. 3D Optic Nerve Head Segmentation in Idiopathic Intracranial Hypertension. In: Tolxdorff T, Deserno TM, Handels H, Meinzer H-P. Bildverarbeitung für die Medizin 2012 [Internet]. Springer Berlin Heidelberg; 2012 [zitiert 7. August 2012]. Seite 262–7. Verfügbar unter: http://www.springerlink.com/content/p551004423q6131w/abstract/

22. Henderson APD, Trip SA, Schlottmann PG, et al. An investigation of the retinal nerve fibre layer in progressive multiple sclerosis using optical coherence tomography. Brain. 2008;131:277–87.

23. Pulicken M, Gordon-Lipkin E, Balcer LJ, Frohman E, Cutter G, Calabresi PA. Optical coherence tomography and disease subtype in multiple sclerosis. Neurology. November 2007;69:2085–92.

24. Dörr J, Radbruch H, Bock M, et al. Encephalopathy, visual disturbance and hearing loss—recognizing the symptoms of Susac syndrome. Nat Rev Neurol. 2009;5:683–8.

25. Kupersmith MJ, Gamell L, Turbin R, Peck V, Spiegel P, Wall M. Effects of weight loss on the course of idiopathic intracranial hypertension in women. Neurology. 1998;50:1094–8.

8. Eidesstattliche Versicherung

„Ich, Falko Andreas Kaufhold, versichere an Eides statt durch meine eigenhändige Unterschrift, dass ich die vorgelegte Dissertation mit dem Thema: „Der Stellenwert der optischen Kohärenztomografie in der Diagnostik und Differentialdiagnostik von Erkrankungen des zentralen Nervensystems“ selbstständig und ohne nicht offengelegte Hilfe Dritter verfasst und keine anderen als die angegebenen Quellen und Hilfsmittel genutzt habe.
Alle Stellen, die wörtlich oder dem Sinne nach auf Publikationen oder Vorträgen anderer Autoren beruhen, sind als solche in korrekter Zitierung kenntlich gemacht. Die Abschnitte zu Methodik (insbesondere praktische Arbeiten, Laborbestimmungen, statistische Aufarbeitung) und Resultaten (insbesondere Abbildungen, Graphiken und Tabellen) entsprechen den URM und werden von mir verantwortet.
Meine Anteile an den ausgewählten Publikationen entsprechen denen, die in der untenstehenden gemeinsamen Erklärung mit dem/der Betreuer/in, angegeben sind.
Sämtliche Publikationen, die aus dieser Dissertation hervorgegangen sind und bei denen ich Autor bin, entsprechen den URM und werden von mir verantwortet.
Die Bedeutung dieser eidesstattlichen Versicherung und die strafrechtlichen Folgen einer unwahren eidesstattlichen Versicherung (§156,161 des Strafgesetzbuches) sind mir bekannt und bewusst.“

Datum Falko Andreas Kaufhold

9. Erklärung über Anteil an Publikationen

Der Promovend Falko Kaufhold hat folgenden Anteil an den im Rahmen dieser Promotion vorgelegten Studien:

Publikation 1:
Kaufhold F, Kadas EM, Schmidt C, Kunte H, Hoffmann J, Zimmermann H, Oberwahrenbrock T, Harms L, Polthier K, Brandt AU, Paul F (2012).
Optic Nerve Head Quantification in Idiopathic Intracranial Hypertension by Spectral Domain OCT. PLoS ONE 7(5): e36965.
IF: 4.092 (2011)
Anteil: 65 %
Bei dieser Publikation war ich am Entwurf, sowie der Planung der Studie beteiligt. Die Messungen mittels optischer Kohärenztomographie führte ich selbstständig durch. Daraufhin erstellte ich aus den erhobenen Parametern eine Datenbank und führte die statistische Analyse mittels SPSS unter Supervision durch. Weiterhin schrieb ich den ersten Manuskriptentwurf, führte Überarbeitungen durch, reichte die Arbeit ein und bearbeitete die Fragen und Anmerkungen der Reviewer.

Publikation 2:
Brandt AU, Zimmermann H, **Kaufhold F**, Promesberger J, Schippling S, Finis D, Aktas O, Geis C, Ringelstein M, Ringelstein EB, Hartung HP, Paul F, Kleffner I, Dörr J (2012).
Patterns of Retinal Damage Facilitate Differential Diagnosis between Susac Syndrome and MS. PLoS ONE 7(6): e38741.
IF: 4.092 (2011)
Anteil: 20 %
Im Rahmen dieser Studie führte ich einen Teil der Messungen mittels optischer Kohärenztomographie durch. Weiterhin war ich beteiligt an der Erstellung der Datenbank zur Auswertung der gemessenen Parameter, der Überarbeitung des Manuskripts und der Bearbeitung der Anmerkungen der Reviewer.

Publikation 3:
Oberwahrenbrock T, Schippling S, Ringelstein M, **Kaufhold F**, Zimmermann H, Keser N, Young KL, Harmel J, Hartung HP, Martin R, Paul F, Aktas O, Brandt AU (2012).

Retinal Damage in Multiple Sclerosis Disease Subtypes Measured by High-Resolution Optical Coherence Tomography. Multiple Sclerosis International. 2012;2012:1–10.
IF: kein Impact Factor 2011
Anteil: 15%
Bei diesem Projekt war ich an einem Teil der OCT-Untersuchungen, sowie an der Erstellung einer Datenbank beteiligt. Weiterhin bestand meine Aufgabe in der kritischen Überarbeitung des Manuskripts.

Prof. Dr. med. Friedemann Paul Falko Andreas Kaufhold

10. Originalarbeiten

Publikation 1:

Kaufhold F, Kadas EM, Schmidt C, Kunte H, Hoffmann J, Zimmermann H, Oberwahrenbrock T, Harms L, Polthier K, Brandt AU, Paul F (2012).
Optic Nerve Head Quantification in Idiopathic Intracranial Hypertension by Spectral Domain OCT. PLoS ONE 7(5): e36965.
IF: 4.092 (2011)

Publikation 2:

Brandt AU, Zimmermann H, **Kaufhold F**, Promesberger J, Schippling S, Finis D, Aktas O, Geis C, Ringelstein M, Ringelstein EB, Hartung HP, Paul F, Kleffner I, Dörr J (2012).
Patterns of Retinal Damage Facilitate Differential Diagnosis between Susac Syndrome and MS. PLoS ONE 7(6): e38741.
IF: 4.092 (2011)

Publikation 3:

Oberwahrenbrock T, Schippling S, Ringelstein M, **Kaufhold F**, Zimmermann H, Keser N, Young KL, Harmel J, Hartung HP, Martin R, Paul F, Aktas O, Brandt AU (2012).
Retinal Damage in Multiple Sclerosis Disease Subtypes Measured by High-Resolution Optical Coherence Tomography. Multiple Sclerosis International. 2012;2012:1–10.
IF: kein Impact Factor 2011

OPEN ACCESS Freely available online

PLoS one

Optic Nerve Head Quantification in Idiopathic Intracranial Hypertension by Spectral Domain OCT

Falko Kaufhold[1], Ella Maria Kadas[1], Christoph Schmidt[2], Hagen Kunte[3], Jan Hoffmann[3], Hanna Zimmermann[1], Timm Oberwahrenbrock[1], Lutz Harms[3,4], Konrad Polthier[5], Alexander U. Brandt[1☯], Friedemann Paul[1,4*☯]

1 NeuroCure Clinical Research Center and Experimental and Clinical Research Center, Charité – Universitätsmedizin Berlin and Max Delbrück Center for Molecular Medicine, Berlin, Germany, **2** Institute of Neuroradiology, Charité – Universitätsmedizin Berlin, Berlin, Germany, **3** Department of Neurology, Charité – Universitätsmedizin Berlin, Berlin, Germany, **4** Clinical and Experimental Multiple Sclerosis Research Center, Charité – Universitätsmedizin Berlin, Berlin, Germany, **5** Mathematical Geometry Processing Group, Freie Universität Berlin, Berlin, Germany

Abstract

Objective: To evaluate 3D spectral domain optical coherence tomography (SDOCT) volume scans as a tool for quantification of optic nerve head (ONH) volume as a potential marker for treatment effectiveness and disease progression in idiopathic intracranial hypertension (IIH).

Design and Patients: Cross-sectional pilot trial comparing 19 IIH patients and controls matched for gender, age and body mass index. Each participant underwent SDOCT. A custom segmentation algorithm was developed to quantify ONH volume (ONHV) and height (ONHH) in 3D volume scans.

Results: Whereas peripapillary retinal nerve fiber layer thickness did not show differences between controls and IIH patients, the newly developed 3D parameters ONHV and ONHH were able to discriminate between controls, treated and untreated patients. Both ONHV and ONHH measures were related to levels of intracranial pressure (ICP).

Conclusion: Our findings suggest 3D ONH measures as assessed by SDOCT as potential diagnostic and progression markers in IIH and other disorders with increased ICP. SDOCT may promise a fast and easy diagnostic alternative to repeated lumbar punctures and could therefore ease monitoring of treatment or disease progression.

Citation: Kaufhold F, Kadas EM, Schmidt C, Kunte H, Hoffmann J, et al. (2012) Optic Nerve Head Quantification in Idiopathic Intracranial Hypertension by Spectral Domain OCT. PLoS ONE 7(5): e36965. doi:10.1371/journal.pone.0036965

Editor: Martin Stangel, Hannover Medical School, Germany.

Received December 21, 2011; **Accepted** April 11, 2012; **Published** May 15, 2012

Funding: The study was supported by a grant from the German Research Foundation (DFG Exc. 257) and a grant from the German Secretary of Economics (BMWi, ZIM KF2286101FO9). The funders had no role in study design, data collection and analysis, decision to publish, or preparation of the manuscript.

Competing Interests: The authors have declared that no competing interests exist.

* E-mail: friedemann.paul@charite.de

☯ These authors contributed equally to this work.

Introduction

Idiopathic intracranial hypertension (IIH), also known as pseudotumor cerebri (PTC), is a clinical syndrome of unknown etiology characterized by increased intracranial pressure (ICP) which typically affects young, obese women of childbearing age [1–5]. Clinical symptoms include headache, visual disturbances, pulsating tinnitus, photopia, eye pain, diplopia and nausea. Papilledema with subsequent visual field loss is the most feared clinical consequence, which mainly determines the therapy and outcome of the syndrome [6–9]. However, although detection of papilledema by an experienced ophthalmologist is a powerful tool in primary diagnosis, it remains a limited method in producing quantitative data to evaluate longitudinal optic disc changes in patients with IIH [10,11].

Optical coherence tomography (OCT) is a non-invasive imaging method, which creates in vivo cross-sectional patterns of the retina [12]. In recent years, OCT has become a valuable tool for assessing retinal axonal damage in several neurological diseases such as optic neuritis, multiple sclerosis, neuromyelitis optica, spinocerebellar ataxia, and Parkinson's disease [13–20]. Moreover, OCT is associated both with morphologic and metabolic changes in brain, thus providing an easy accessible window into the brain in neurologic diseases [21–23].

Few studies investigated OCT in IIH using the retinal nerve fiber layer thickness (RNFLT) in a peripapillary ring scan as outcome parameter. Patients with newly diagnosed IIH presented RNFL thickening compared to healthy controls, which decreased after three months under IIH treatment, thus proposing RNFLT as a potential longitudinal measure [24–26]. Subsequently it was shown, that peripapillary RNFLT swelling due to increased ICP correlates well with optic disc elevation or papilledema in funduscopy [27]. However, all these studies used 2D time domain OCT that does not allow direct 3D measurement of the optic nerve head (ONH). Consequently, the peripapillary RNFLT measurement is only a rough estimate of ONH changes as it is located at the marginal zone of the pathologic process.

Next generation 3D spectral-domain OCT (SDOCT) potentially allows direct ONH quantification and has therefore been proposed for evaluation of papilledema in IIH [28]. However, ONH changes in patients with IIH (i.e. swelling) impede the use of existing algorithms focusing on other diseases [29]. For this reason we developed a novel custom segmentation algorithm using an extension of the retinal pigment epithelium through the ONH as reference line, which enabled us to automatically assess ONH volume and shape in IIH patients that should also be applicable in other diseases with elevated ICP and optic disc swelling.

Next, in a prospective cross-sectional pilot study we aimed to quantify ONH differences by SDOCT between IIH patients and matched controls. Lastly, we investigated a possible association between SDOCT measures and clinical data which would be relevant for the question whether ONH quantification may serve as a tool for monitoring disease progression and therapeutic effects in IIH.

Methods

Patients and Participants

The study included patients with a minimum age of 18 years and a definite diagnosis of IIH according to the modified Dandy criteria [30]. Patients were consecutively recruited from the neurology outpatient clinic at the Charité- Universitätsmedizin Berlin between June 2010 and July 2011. Exclusion criteria were systemic conditions or medication affecting ICP other than IIH related medication, pregnancy or postpartum period, surgical interventions affecting cerebro-spinal fluid circulation (e.g. shunting procedures or fenestration of the optic nerve sheath) and an ophthalmological disease which could influence OCT imaging (i.e. glaucoma).

All patients received a complete neurological examination supervised by a board certified neurologist. The following data were compiled: disease duration, current body mass index (BMI), most recent lumbar puncture opening pressure (latest ICP), current medical treatment and current IIH symptoms (i.e. headache, visual obscurations, tinnitus, dizziness, nausea). For measurement of ICP patients were lying on their right side in a fetal position. After the subarachnoid space was punctured, cerebrospinal fluid opening pressure was determined by the means of a column manometer. A cohort of age, gender and BMI matched controls was recruited among employees and obese patients from the psychosomatic medicine department of the Charité- Universitätsmedizin Berlin, which were treated only for adiposity. Symptoms of increased ICP as well as a diagnosis of IIH were ruled out clinically in the control group by board certified neurologists. The same exclusion criteria and examinations of the patient group applied to the control group (CG). The study was approved by the local ethics committee of the Charité- Universitätsmedizin Berlin and was conducted in accordance to the Declaration of Helsinki in its currently applicable version, the guidelines of the International Conference on Harmonisation of Good Clinical Practice (ICH-GCP) and the applicable German laws. All participants gave informed written consent.

Optical Coherence Tomography

RNFLT, total macular volume (TMV) and 3D ONH scans were obtained using a spectral-domain OCT (Heidelberg Spectralis SDOCT, Heidelberg Engineering, Germany, Spectralis software version 5.3.3.0, Eye Explorer software 1.6.4.0) for each eye of the patients and matched controls. RNFLT was measured using a 3.4 mm circular scan around the ONH with the device's standard protocol and segmentation algorithm with activated eye tracker (TrueTrack®) and the maximum number of averaging frames in ART–MEAN mode was tried to achieve. TMV was measured by a custom protocol which generated 61 slices (B-scans) focusing the fovea centralis with a scanning angle of $30^\circ \times 25^\circ$ and a resolution of 768 A-scans per B-scan. TMV was calculated by estimating the distance between the inner limiting membrane and the Bruch-membrane in a cylinder with 6 mm in diameter using the device software's segmentation algorithm. The 3D ONH scan was performed using a custom protocol with 145 slices (B-scans), focusing the optic nerve head with a scanning angle of $15^\circ \times 15^\circ$ and a resolution of 384 A-scans per B-scan.

All scans were acquired by one of three experienced operators and were reviewed for sufficient signal strength, correct centering and segmentation by an independent operator not involved in the study. All operators were blinded towards patient and control groups; however, due to the nature of papilledema patients could be easily identified in most cases by ONH images alone.

3D Optic Nerve Head Analysis

For the automatic assessment of ONH changes we developed a custom and fully automatic algorithm that measures the volume (ONHV) and maximum height (ONHH) of the disc edema. A detailed description of the algorithm including reliability and validation analyses is published elsewhere [31]. In brief, ONH OCT scans tend to have regions of strong varying intensity values caused by the edema. Additionally, scans are characterized by an increased intrinsic speckle noise making a reliable differentiation of intra retinal layers challenging to impossible. This algorithm identifies and uses two reference boundaries on each B-scan, the inner limiting membrane (ILM) and a hypothetical extension of the peripapillary retinal pigment epithelium (RPE) through the ONH. The edema is then defined as the area enclosed by these two layers. The ILM is provided in sufficient quality by the device's segmentation software. In order to compute the volume and maximal height of the edema the algorithm focuses on segmenting the RPE to create a base area for further calculation of both parameters. First an initial region that contains this layer is estimated. Starting from this region, unnecessary pixels are discarded. The RPE curve, describing the layer, is obtained by a fully automatic least square spline fitting of 2nd or 3rd order depending on the number of detected RPE segments. Furthermore, to account for the natural retinal curvature seen in SDOCT images, we performed an image flattening on each slice using again the RPE, followed by the final volume and height computation. For the volume measurement a threshold of 20 pixels was applied from the reference height computed at the right side and left side of each flattened B-scan. The area of the edema found on each B-scan multiplied by the special spacing was summed up to obtain the final volume. This threshold was selected to include most of the ONH and to provide a satisfying volume of the swelling in IIH as well as healthy controls. An overview of the segmentation algorithm is shown in figure 1.

For algorithm development and application, 3D images were exported from the SDOCT device and imported into Matlab using a custom import filter based on documentation provided by the device manufacturer. Development was performed using Matlab R2011A with additional library Spline (Mathworks, Ismaning, Germany).

Statistical Analysis

Differences between the two study groups were analyzed by independent samples Mann-Whitney U test for age and BMI. For evaluation of the relationship between RNFLT, TMV, ONH parameters and clinical data, we performed generalized estimation

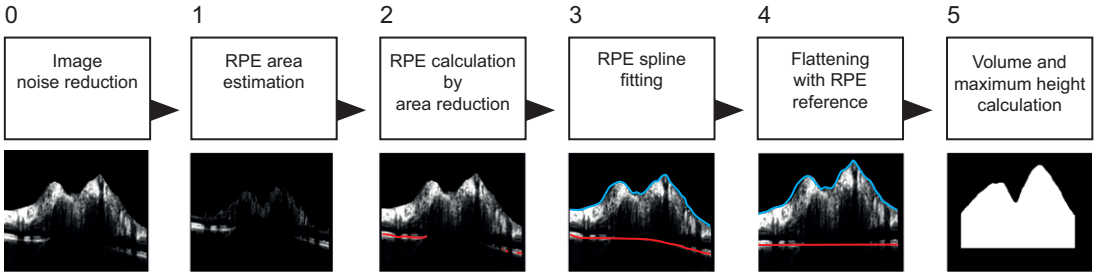

Figure 1. Overview of the custom segmentation process for assessing ONH volume and height in IIH patients. 0) First OCT B scans are cleaned from noise and smoothed, 1) then the area in which the RPE is expected is narrowed by removing bright upper layers of the scan, resulting in the brightest spots belonging most likely to the RPE. 2) From the A scan at the first quarter and the A scan at the last quarter of the B scan, the possible RPE area is further reduced by detecting the brightest spots of the image (red lines). 3) On the proposed RPE candidates a least square spline approximation is applied (red line), resulting in a hypothetical RPE through the ONH. The ILM is provided from the device's segmentation software (blue line). 4) The scans are flattened using the RPE as reference. 5) Finally volume and height are calculated in the newly defined area.
doi:10.1371/journal.pone.0036965.g001

equation (GEE) analyses with working correlation matrix structure "exchangeable" accounting for inter-eye/intra-patient dependencies. Clinical parameters (diagnosis and treatment) were used as independent and RNFLT, TMV or ONH parameters as dependent variables. Correlation of RNFLT with ONHH or ONHV was analyzed using Spearman's Rho.

For identifying a possible relationship of ICP with ONHH or ONHV we included only patients with an interval between ICP and OCT measurements of less than 24 months (n = 11) and additionally weighted data in GEE models with ICP as the independent variable and either ONHH or ONHV as the dependent variable by factor $\omega = 100/(\text{measurement distance in months}+1)$. Hereby, OCT scans closer to the ICP measurements are more strongly weighted in the subsequent analysis, whereas scans with a longer interval are weighted less.

Reliability of ONHH and ONHV was determined using intra-class correlation coefficient on repeated measurements using the two-way mixed effects model where subject effects are random and measures effects are fixed.

RNFLT percentiles for comparison with normal values are given from the OCT device's internal normative database. All statistical analyses were performed with SPSS 19 (IBM SPSS Statistics Version 19, Release 19.0.0.1, IBM, Armonk, NY, USA). Statistical significance was established at $p<0.05$ in all analyses. All tests should be understood as exploratory data analysis, in that no previous power calculation and adjustments for multiple testing were performed.

Table 1. Demographic overview of IIH patients and controls.

	Parameter	Patients	Controls
N		19	19
Age (years)	Mean ± SD	38.0±13.8	37.6±12.9
	Min–Max	20–63	20–61
Gender (female/male)	N/N	17 / 2	17 / 2
BMI (kg/m^2)	Mean ± SD	33.6±7.4	33.8±7.3
	Min–Max	24.1–54.6	24.8–48.1
Disease duration (months)	Mean ± SD	40±37	-
	Min–Max	0–115	-
Latest ICP (cmH_2O)	Mean ± SD	28.6±6.3	-
	Min–Max	18.0–40.0	-
Time since last ICP (months)	Mean ± SD	20±20	-
	Min–Max	0–57	-

Abbreviations: IIH = idiopathic intracranial hypertension; ICP = intracranial pressure; SD = standard deviation; Min = minimum value; Max = maximum value.
doi:10.1371/journal.pone.0036965.t001

Results

Cohort description

This study enrolled 37 eyes from 19 IIH patients and 38 eyes from 19 matched controls. One IIH eye had to be excluded due to newly diagnosed epiretinal membranes. Demographics of patients and controls are displayed in table 1. Patients and controls did not differ regarding gender, age and BMI. Headache (84%) was the most common symptom in IIH patients. Furthermore, all patients suffered from at least one of the following visual symptoms during the course of their disease: photopsia (79%), photophobia (58%), blurred vision (42%) and visual acuity loss (26%). They also described dizziness (58%), tinnitus (37%) and nausea (37%). Thirteen patients were treated pharmacologically with either acetazolamide (n = 11), topiramate (n = 1) or furosemide (n = 1) at the time of OCT measurement.

RNFLT and TMV differences

We found no significant differences in average RNFLT and TMV between IIH patients and CG (table 2). Although overall group differences were not significant, seven eyes from four IIH patients showed abnormally high RNFLT values above the 95th percentile.

Reliability of ONH measurements and quantification

To determine the reliability of ONHV and ONHH, each eye was measured three times in a row in 3 patients (6 eyes). Each measurement was then post-processed in a fully automated fashion using the presented algorithm. ICC for ONHV was 0.999 ($p<0.001$) and ICC for ONHH was 0.983 ($p<0.001$).

ONH volume and height differences

ONHV in patients was increased compared to controls ($p<0.001$, table 2 and figure 2C). Furthermore, 18 eyes from 11 IIH

Table 2. Comparison of optical coherence tomography measurements between IIH patients and controls.

	Patients		Controls		GEE
	Mean ± SD	Min–Max	Mean ± SD	Min–Max	
RNFLT (μm)	99.1±18.1	58.4–155.5	99.2±8.0	79.9–111.9	P = 0.942
TMV (mm^3)	8.48±0.40	7.72–9.01	8.67±0.38	7.87–9.28	P = 0.141
ONHV (mm^3)	2.30±1.25	0.41–5.97	1.08±0.49	0.28–2.17	**p<0.001**
					B = 1.2; SE = 0.3
ONHH (mm)	0.42±0.07	0.34−0.64	0.40±0.03	0.34−0.46	P = 0.099

Abbreviations: RNFLT = retinal nerve fiber layer thickness; TMV = total macular volume; ONHV = optic nerve head volume; ONHH = optic nerve head height; SD = standard deviation; Min = minimum value; Max = maximum value; GEE = generalized estimating equation models analyses accounting for inter–eye/intra-patient dependencies; B = regression coefficient; SE = coefficient standard error; p = p value.

doi:10.1371/journal.pone.0036965.t002

patients showed an ONHV above the 95th percentile of the CG (ONHV = 2.09 mm^3). ONHH did not differ between groups (table 2). Two sample 3D ONH scans from a control subject and an IIH patient are given in figure 2A and B. A receiver operating characteristic analysis (ROC) between IIH patients and controls presented a much higher area under the curve for ONHV (AUC = 0.835) than for RNFLT (AUC = 0.464).

We further divided the patient group into treated and untreated patients. Untreated patients (n = 6) showed a higher ONHV than treated (n = 13) patients (GEE, p<0.001, table 3 and figure 2D). Both medically treated and untreated patients had an increased ONHV compared to controls which did not hold true for ONHH. Additionally all but one eye from untreated patients showed an ONHV above the 95th percentile of the CG. RNFLT analysis of the subgroups displayed also an increase for untreated patients (GEE, p = 0.03, table 3).

In a Spearman's Rho analysis in IIH patients only, RNFLT correlated both with ONHV (r = 0.501, p<0.001) and ONHH (r = 0.482, p = 0.003).

Association of ICP with ONH volume and height

Lastly, we assessed the association of ONH measures and ICP. Since the pilot trial design prohibited a direct measurement of ICP next to OCT, we deployed the latest measured lumbar puncture opening pressure, weighting it for the distance of measurement as described in methods and including only patients with ICP measurements closer to 24 months from OCT (n = 11).

Using this approach, GEE with ICP as the independent variable weighted for distance of measurement and ONHV or ONHH as the dependent variable were weakly significant for ONHV (B = 0.020, SE = 0.007, p = 0.004) and interestingly significant for ONHH with a negative association (B = −0.003, SE = 0.0005, p<0.001), meaning that IIH patients with a high ICP showed a more depressed ONHH.

Discussion

In this pilot study we examined IIH patients and matched controls using 3D SDOCT with a novel segmentation algorithm to assess optic nerve head changes. Our main findings are: (a) ONH volume was increased in IIH vs. CG and (b) in untreated versus treated patients. (c) In contrast, neither RNFLT nor TMV differed between IIH patients and controls, although a few patients showed very high RNFLT values. (d) ONHV was weakly associated with ICP, while ONHH showed an inverse association. Finally, (e) a substantially higher proportion of IIH patients exhibited ONHV values above the 95th percentile of controls (18 eyes of 11 patients, 57.9%, including all 6 untreated patients) as compared to RNFLT (7 eyes of 4 patients, 21.0%) which indicates a higher susceptibility of 3D ONH changes to alterations in ICP than RNFLT. ONH volume showed a significant increase even in those IIH patients in whom RNFLT remained normal. Thus, automated analysis of ONH shape may present a first step towards detecting even marginal changes in the composition of optic disc swelling. The necessity of quantitative evaluation of the optic disc was recently emphasized by another clinical study using transorbital sonography to follow IIH patients around lumbar puncture to create a more valuable tool for disease monitoring [32]. This study investigated especially the 2D sonographic parameters optic nerve sheath diameter (OSND), optic nerve diameter (OND) and optic disc elevation. OSND was significantly increased in IIH patients before lumbar puncture and decreased hereafter, while OND showed no differences to controls. The penetration depth of OCT disallows an evaluation of the optic disc sheath. On the other hand SDOCT could detect morphological changes of the ONH and its boundaries in more detail, because of the much higher resolution than transorbital sonography (OCT optic resolution: 7 μm axial and 14 μm lateral; sonographic resolution in millimeter range). Thus, in the future both methods with their respective advantages and limitations may complement each other in improving assessment of the optic nerve head and sheath in IIH and other conditions associated with increased ICP.

Our findings disclose several possibilities for using quantified ONHV in practice. OCT could aid in new diagnosis of IIH, providing an easy tool to quantify ONH swelling in patients with unclear symptoms. Even if high inter-individual differences in ONH shape limit usage in cross-sectional applications, assessing changes in ONH might prove highly useful in longitudinal settings: Automated 3D ONH assessment could be potentially used for monitoring treatment effectiveness or for quantifying disease progression. This aspect is supported by the higher ONHV in pharmacologically untreated patients.

Of interest in this regard is the inverse association of ONH maximal height and ICP: IIH patients with higher ICP show less pronounced ONH height than patients with lower ICP. These results suggest, that an ONH swelling process occurs more in a plane base than in height, proposing ONHV as the more meaningful parameter of ONH quantification. In addition a wall at the rim of the optic disc is a non-pathological finding also in healthy controls, which could influence the investigative power of ONHH, because the rim is also detected by the algorithm assessing ONHH. One could also speculate that this inverse association is the result from damage to the RNFL occurring during high-pressure phases. The assumption of RNFL damage as a consequence of high ICP and papilledema is supported by the fact that some of our patients showed reduced RNFL. However, due to the sometimes long interval between ICP and OCT measurements this result should be interpreted with caution.

In our study we could not approve the previously published results of RNFLT differences between IIH patients and matched controls in time domain OCT [24]. This might be explained in part by differences in study design: First, we did not involve patients with a newly confirmed IIH. The much longer disease

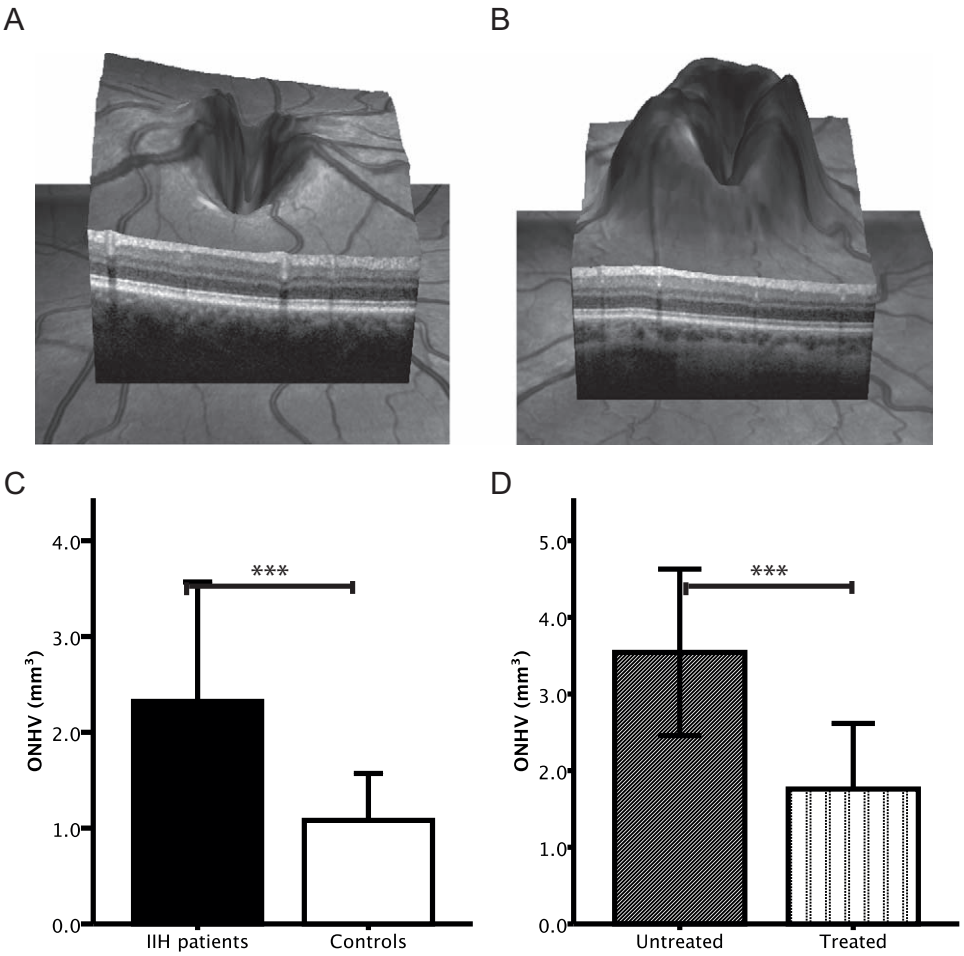

Figure 2. ONH volume and height differences between IIH patients and controls. A) 3D spectral domain OCT ONH measurement from a matched control ONH **B**) 3D spectral domain OCT ONH measurement from an IIH patient with a diagnosed papilledema **C**) Groups differences in optic nerve head volume (ONHV) between IIH patients (black bar) and controls (white bar). **D**) Group difference in ONHV between medically untreated (gray bar) and treated (vertical lines bar) IIH patients. Error bars represent 1x standard deviation in figures c and d. = $p < 0.001$.
doi:10.1371/journal.pone.0036965.g002

duration and treatment of our patient cohort could have a downsizing effect on the measured RNFLT. This is supported by a follow-up study to the above-mentioned trial that identified a significant decrease in disc swelling as detected by OCT after three months of disease duration and treatment [25]. Second, peripapillary RNFLT is limited in describing optic disc swelling because it measures the boundaries of the process only indirectly. In contrast, our study directly quantified papilledema by a novel analysis algorithm, which enables the investigator to gain more detailed information about ONH swelling itself. Although our patients still

Table 3. Subgroup analysis of OCT measurements in medically treated and untreated IIH patients.

	untreated (n = 11 eyes)		treated (n = 26 eyes)		GEE
	Mean±SD	Min–Max	Mean ± SD	Min–Max	
RNFLT (μm)	112.5±19.2	90.3–155.5	93.4±14.5	58.4–120.5	**p = 0.030**
					B = 17.6; SE = 8.1
TMV (mm^3)	8.41±0.34	7.8–8.9	8.51±0.43	7.72–9.01	p = 0.720
ONHV (mm^3)	3.57±1.13	1.6−6.0	1.76±0.86	0.41–4.22	**p<0.001**
					B = 1.8; SE = 0.4
ONHH (μm)	0.46±0.09	0.37−0.64	0.40±0.05	0.34−0.57	p = 0.055

Abbreviations: RNFLT = retinal nerve fiber layer thickness; TMV = total macular volume; ONHV = optic nerve head volume; ONHH = optic nerve head height; SD = standard deviation; Min = minimum value; Max = maximum value; GEE = generalized estimating equation models analyses accounting for inter-eye/intra-patient dependencies; B = regression coefficient; SE = coefficient standard error; p = p value.
doi:10.1371/journal.pone.0036965.t003

had detectable changes in OCT using this ONH analysis, these changes were just not prominent enough to show in RNFLT. Third, some of the patients in this study even showed pronounced RNFL loss, leading i.e. to an AUC of <0.5. We presume, that this RNFL thinning could be a consequence of the high ICP for years, causing neuroaxonal damage and loss [33,34].

Unfortunately it was not possible to perform ICP and OCT measurements at the same time in this pilot trial, which is also the greatest limitation of our study. The significant association of ICP with ONHV when weighting for ICP measurement time distance from OCT points towards a possible direct correlation between ICP and ONH shape. However, these results should be interpreted with care: Since scaling of the weighting variable is unknown and was thus selected arbitrarily, the used statistical model might not be applicable. Confirmation of these results is therefore highly warranted in controlled trials merging time points of ICP and OCT measurements.

Our study points out the urgent need for specialized analysis protocols for neurologic diseases using OCT. Although OCT's informative value is limited to the retina, its value in combination with powerful and specialized software for applications in neurology can be greatly improved. Overall, the detection of the optic disc volume and height makes SDOCT in combination with the newly developed segmentation algorithm a valuable tool for evaluating papilledema in IIH patients. The custom segmentation method should be further developed for and applied in follow-up trials to determine reliability, precision and ultimately diagnostic value with sensitivity and specificity. Further statistical optimization could e.g. be achieved by combining information from both eyes into differential diagnosis models.

In summary, our findings suggest ONH volume scans as a diagnostic and progression parameter in IIH with higher sensitivity to ICP changes than RNFLT. OCT is a fast and inexpensive method. A typical examination does not exceed 10 minutes per eye. Thus, OCT could promise a fast and easy alternative to repeat lumbar punctures, exercised in Europe to follow IIH patients, and could therefore ease monitoring of disease progression and treatment response. Furthermore, the methods for quantifying ONH swelling should potentially be applicable in other disorders with elevated intracranial pressure that lead to papilledema.

Author Contributions

Analyzed the data: FK AUB. Wrote the paper: FK AUB. Designed and coordinated the study: FP LH JH HK. Clinically assessed the IIH patients and provided logistical support: HK CS. Performed OCT measurements: FK HZ TO. Developed the custom ONH algorithm: EK KP. Provided important intellectual content in preparation of the trial and the manuscript: FK EMK CS HK JH HZ TO LH KP AUB FP.

References

1. Friedman DI, Jacobson DM (2002) Diagnostic criteria for idiopathic intracranial hypertension. Neurology 59: 1492–1495.
2. Kesler A, Hadayer A, Goldhammer Y, Almog Y, Korczyn AD (2004) Idiopathic intracranial hypertension. Neurology 63: 1737–1739.
3. Wall M (2010) Idiopathic Intracranial Hypertension. Neurol Clin 28: 593–617.
4. Kupersmith MJ, Gamell L, Turbin R, Peck V, Spiegel P, et al. (1998) Effects of weight loss on the course of idiopathic intracranial hypertension in women. Neurology 50: 1094–1098.
5. Ko MW, Chang SC, Ridha MA, Ney JJ, Ali TF, et al. (2011) Weight gain and recurrence in idiopathic intracranial hypertension. Neurology 76: 1564–1567.
6. Ball AK, Clarke CE (2006) Idiopathic intracranial hypertension. The Lancet Neurology 5: 433–442.
7. Friedman DI, Rausch EA (2002) Headache diagnoses in patients with treated idiopathic intracranial hypertension. Neurology 58: 1551–1553.
8. Wong GK, Poon WS Pseudotumor Cerebri: Time to Reflect on Treatment. World Neurosurgery 75: 592–593.
9. Shah VA, Kardon RH, Lee AG, Corbett JJ, Wall M (2008) Long-term follow-up of idiopathic intracranial hypertension. Neurology 70: 634–640.
10. Friedman DI (2004) Pseudotumor cerebri. Neurol Clin 22: 99–131.
11. Wolf A, Hutcheson KA (2008) Advances in evaluation and management of pediatric idiopathic intracranial hypertension. Current Opinion in Ophthalmology 19: 391–397.
12. Huang D, Swanson EA, Lin CP, Schuman JS, Stinson WG, et al. (1991) Optical coherence tomography. Science 254: 1178–1181.
13. Costello F, Coupland S, Hodge W, Lorello GR, Koroluk J, et al. (2006) Quantifying axonal loss after optic neuritis with optical coherence tomography. Annals of Neurology 59: 963–969.
14. Petzold A, de Boer JF, Schippling S, Vermersch P, Kardon R, et al. (2010) Optical coherence tomography in multiple sclerosis: a systematic review and meta-analysis. Lancet Neurol 9: 921–932.
15. Burkholder BM, Osborne B, Loguidice MJ, Bisker E, Frohman TC, et al. (2009) Macular Volume Determined by Optical Coherence Tomography as a Measure of Neuronal Loss in Multiple Sclerosis. Arch Neurol 66: 1366–1372.
16. Bock M, Brandt AU, DÃ¶rr J, Kraft H, Weinges-Evers N, et al. (2010) Patterns of retinal nerve fiber layer loss in multiple sclerosis patients with or without optic neuritis and glaucoma patients. Clinical Neurology and Neurosurgery 112: 647–652.
17. Ratchford JN, Quigg ME, Conger A, Frohman T, Frohman E, et al. (2009) Optical coherence tomography helps differentiate neuromyelitis optica and MS optic neuropathies. Neurology 73: 302–308.
18. de Seze J, Blanc F, Jeanjean L, Zephir H, Labauge P, et al. (2008) Optical Coherence Tomography in Neuromyelitis Optica. Arch Neurol 65: 920–923.
19. Stricker S, Oberwahrenbrock T, Zimmermann H, Schroeter J, Endres M, et al. (2011) Temporal retinal nerve fiber loss in patients with spinocerebellar ataxia type 1. PLoS ONE 6: e23024.
20. Moschos MM, Tagaris G, Markopoulos I, Margetis I, Tsapakis S, et al. (2011) Morphologic changes and functional retinal impairment in patients with Parkinson disease without visual loss. Eur J Ophthalmol 21: 24–29.
21. Gordon-Lipkin E, Chodkowski B, Reich DS, Smith SA, Pulicken M, et al. (2007) Retinal nerve fiber layer is associated with brain atrophy in multiple sclerosis. Neurology 69: 1603–1609.
22. Pfueller CF, Brandt AU, Schubert F, Bock M, Walaszek B, et al. (2011) Metabolic Changes in the Visual Cortex Are Linked to Retinal Nerve Fiber Layer Thinning in Multiple Sclerosis. PLoS ONE 6: e18019.
23. Dörr J, Wernecke KD, Bock M, Gaede G, Wuerfel JT, et al. (2011) Association of Retinal and Macular Damage with Brain Atrophy in Multiple Sclerosis. PLoS ONE 6: e18132.
24. Skau M, Milea D, Sander B, Wegener M, Jensen R (2010) OCT for optic disc evaluation in idiopathic intracranial hypertension. Graefes Arch Clin Exp Ophthalmol 249: 723–730.
25. Skau M, Sander B, Milea D, Jensen R (2010) Disease activity in idiopathic intracranial hypertension: a 3-month follow-up study. J Neurol 258: 277–283.
26. Yri HM, Wegener M, Sander B, Jensen R (2006) Idiopathic intracranial hypertension is not benign: a long-term outcome study. Journal of Neurology. Available: http://www.springerlink.com/content/mmkj64211w254h54/. Accessed 2 December 2011.
27. Waisbourd M, Leibovitch I, Goldenberg D, Kesler A (2007) OCT assessment of morphological changes of the optic nerve head and macula in idiopathic intracranial hypertension. Clinical Neurology and Neurosurgery In Press, Corrected Proof. Available: http://www.sciencedirect.com/science/article/pii/S0303846711001661. Accessed 11 August 2011.
28. Heidary G, Rizzo JF (2010) Use of Optical Coherence Tomography to Evaluate Papilledema and Pseudopapilledema. Semin Ophthalmol 25: 198–205.
29. Strouthidis NG, Fortune B, Yang H, Sigal IA, Burgoyne CF (2011) Longitudinal Change Detected by Spectral Domain Optical Coherence Tomography in the Optic Nerve Head and Peripapillary Retina in Experimental Glaucoma. Investigative Ophthalmology & Visual Science 52: 1206–1219.
30. Smith JL (1985) Whence pseudotumor cerebri? J Clin Neuroophthalmol 5: 55–56.
31. Kadas EM, Kaufhold F, Schulz C, Paul F, Polthier K et al (2012) 3D optic nerve head segmentation in idiopathic intracranial hypertension. Bildverarbeitung für die Medizin 2012. In press.
32. Bäuerle J, Nedelmann M (2011) Sonographic assessment of the optic nerve sheath in idiopathic intracranial hypertension. Journal of Neurology 258: 2014–2019.
33. Wall M, George D (1991) IDIOPATHIC INTRACRANIAL HYPERTENSION. Brain 114A: 155–180.
34. Gu XZ, Tsai JC, Wurdeman A, Wall M, Foote T, et al. (1995) Pattern of axonal loss in longstanding papilledema due to idiopathic intracranial hypertension. Curr Eye Res 14: 173–180.

OPEN ACCESS Freely available online

PLoS one

Patterns of Retinal Damage Facilitate Differential Diagnosis between Susac Syndrome and MS

Alexander U. Brandt[1], Hanna Zimmermann[1], Falko Kaufhold[1], Julia Promesberger[2], Sven Schippling[3], David Finis[4], Orhan Aktas[5], Christian Geis[6], Marius Ringelstein[5], E. Bernd Ringelstein[7], Hans-Peter Hartung[5], Friedemann Paul[1,8,9], Ilka Kleffner[7], Jan Dörr[1,8]*

1 NeuroCure Clinical Research Center, Charité – Universitätsmedizin Berlin, Berlin, Germany, **2** Department of Ophthalmology, University of Münster, Münster, Germany, **3** Institute for Neuroimmunology and Clinical Multiple Sclerosis Research (inims), University Medical Center Hamburg Eppendorf, Hamburg, Germany, **4** Department of Ophthalmology, University Medical Center, Heinrich-Heine-University, Düsseldorf, Germany, **5** Department of Neurology, University Medical Center, Heinrich-Heine-University, Düsseldorf, Germany, **6** Department of Neurology, University of Würzburg, Würzburg, Germany, **7** Department of Neurology, University of Münster, Münster, Germany, **8** Clinical and Experimental Research Center for Multiple Sclerosis, Department of Neurology, Charité – Universitätsmedizin Berlin, Berlin, Germany, **9** Experimental and Clinical Research Center, Max Delbrück Center for Molecular Medicine and Charité – Universitätsmedizin Berlin, Berlin, Germany

Abstract

Susac syndrome, a rare but probably underdiagnosed combination of encephalopathy, hearing loss, and visual deficits due to branch retinal artery occlusion of unknown aetiology has to be considered as differential diagnosis in various conditions. Particularly, differentiation from multiple sclerosis is often challenging since both clinical presentation and diagnostic findings may overlap. Optical coherence tomography is a powerful and easy to perform diagnostic tool to analyse the morphological integrity of retinal structures and is increasingly established to depict characteristic patterns of retinal pathology in multiple sclerosis. Against this background we hypothesised that differential patterns of retinal pathology facilitate a reliable differentiation between Susac syndrome and multiple sclerosis. In this multicenter cross-sectional observational study optical coherence tomography was performed in nine patients with a definite diagnosis of Susac syndrome. Data were compared with age-, sex-, and disease duration-matched relapsing remitting multiple sclerosis patients with and without a history of optic neuritis, and with healthy controls. Using generalised estimating equation models, Susac patients showed a significant reduction in either or both retinal nerve fibre layer thickness and total macular volume in comparison to both healthy controls and relapsing remitting multiple sclerosis patients. However, in contrast to the multiple sclerosis patients this reduction was not distributed over the entire scanning area but showed a distinct sectorial loss especially in the macular measurements. We therefore conclude that patients with Susac syndrome show distinct abnormalities in optical coherence tomography in comparison to multiple sclerosis patients. These findings recommend optical coherence tomography as a promising tool for differentiating Susac syndrome from MS.

Citation: Brandt AU, Zimmermann H, Kaufhold F, Promesberger J, Schippling S, et al. (2012) Patterns of Retinal Damage Facilitate Differential Diagnosis between Susac Syndrome and MS. PLoS ONE 7(6): e38741. doi:10.1371/journal.pone.0038741

Editor: Markus Schuelke, Charité Universitätsmedizin Berlin, NeuroCure Clinical Research Center, Germany

Received October 26, 2011; **Accepted** May 9, 2012; **Published** June 11, 2012

Funding: This study was supported in part by Deutsche Forschungsgemeinschaft (DFG Exc. 257). The MS Center at the Department of Neurology, Heinrich-Heine-University Düsseldorf, is supported in part by the Walter-and-Ilse-Rose Stiftung. The Institute for Neuroimmunology and Clinical Multiple Sclerosis Research (inims), University Medical Center Hamburg Eppendorf, Hamburg, is supported in part by Hertie Stiftung. The funders had no role in study design, data collection and analysis, decision to publish, or preparation of the manuscript. No additional external funding was received for this study.

Competing Interests: The authors have declared that no competing interests exist.

* E-mail: jan-markus.doerr@charite.de

Introduction

Susac syndrome is a rare disease characterised by the clinical triad of encephalopathy, vision disturbances, namely visual field defects, and sensorineural hearing loss [1–3]. The exact prevalence of Susac syndrome is unknown, and its pathogenesis is still unclear; autoimmune processes that lead to an occlusion of small vessels in the brain, retina and inner ear are believed to play an important role [4,5]. The disease most often manifests in the third to fourth decade [6]. The prognosis mainly depends on the severity, the often self-limited and monophasic, sometimes fluctuating and rarely relapsing clinical course [7], and the appropriate treatment [8,9]. Retinal infarction presenting with scotoma is one of the clinical hallmarks, although often not predominant. Patients can present with episodic or permanent vision loss [6]. Fluorescein angiography (FAG) and funduscopy show branch retinal artery occlusions (BRAO), arterial wall hyperfluorescence and retinal arterial wall plaques, termed Gass plaques [10]. Retinal involvement can be missed in cases where patients do not complain about visual disturbances due to neuropsychological impairment, or when physicians are not familiar with the disease. In fact, in several reported cases BRAO was only detected after repeated FAG [6].

The diagnosis of Susac syndrome is straightforward, when the characteristic clinical triad is complete, when the physician is familiar with the clinical presentation, and when the crucial diagnostic procedures are carried out and show characteristic findings like BRAO in FAG. However, the diagnosis is often complicated by the fact that the characteristic signs usually do not occur concomitantly but rather develop successively with symptom-free intervals [3], which often enough results in a delayed or even completely missed diagnosis. Consensus criteria for the

Table 1. Demographic overview of Susac patients included in the study.

Subjects	n	9
Eyes	n	18
Gender	Male (%)	3 (33)
	Female (%)	6 (67)
Age (years)	Mean ± SD	33±11
	Min – Max	20–47
Time since diagnosis (months)	Mean ± SD	65±55
	Min – Max	3–173
Encephalopathy	No (%)	1 (11)
	Yes (%)	8 (89)
Hearing loss	No (%)	0 (0)
	Yes (%)	9 (100)
Visual impairment (eyes)	No (%)	3 (17)
	Yes (%)	15 (83)
	No (%)	3 (17)
	Yes (%)	15 (83)

Abbreviations: BRAO = branch retinal artery occlusion, SD = standard deviation.

doi:10.1371/journal.pone.0038741.t001

diagnosis of Susac syndrome have not yet been established. In MRI, Susac syndrome usually presents with "punched-out" lesions, frequently in the corpus callosum and periventricular area [11]. A number of differential diagnoses, most of which occur more frequently than Susac syndrome, have to be taken into consideration [3]. In turn, Susac syndrome should be considered as differential diagnosis in various conditions. Due to some overlap in the clinical presentation and the patterns of MRI pathology multiple sclerosis (MS) is probably the most frequent misdiagnosis of Susac syndrome [2,8,11,12]. However, with respect to the different therapeutic approach, particularly the necessity of a first-line immunosuppressive treatment in Susac syndrome in contrast to primarily immunomodulatory approaches in MS, a prompt establishment of the diagnosis is essential. Additional diagnostic criteria allowing an early differential diagnosis are therefore highly warranted.

Optical coherence tomography (OCT) has recently become a valuable addition to the neurologist's diagnostic toolbox, proving its usefulness in a variety of disorders with neuro-ophthalmologic involvement [13–16]. OCT facilitates e.g. non-invasive quantification of both the thickness of the retinal nerve fibre layer (RNFLT), which represents unmyelinated axons of retinal ganglia converging to the optic disc to form the optic nerve and the macular volume which represents the volume of the central retina [13–16]. In a recently published case report we could demonstrate pathologic OCT findings in a patient with Susac syndrome [3]. Based on these findings we hypothesised that retinal changes (i) can be regularly detected by OCT in patients with Susac syndrome and (ii) differ from retinal pathology observed in MS. A different pattern of retinal pathology in Susac syndrome and MS would be of clinical value in terms of distinguishing patients with Susac syndrome from MS patients.

Methods

Objectives

To identify OCT changes in patients with Susac syndrome and to compare these changes with matched healthy controls and multiple sclerosis patients.

Table 2. Optical coherence tomography data of the nine patients with Susac syndrome.

Pat.	Sex	Age	Dur.	Eye	VS	BRAO	TMV [mm^3]	A [μm]	T [μm]	S [μm]	N [μm]	I [μm]
P1	m	20	26	OD	yes	yes	6.00	85	48	101	70	122
				OS	yes	yes	7.22	83	65	107	47	115
P2	m	32	58	OD	yes	yes	7.64	105	81	132	106	102
				OS	no	yes	7.66	108	77	141	98	115
P3	f	44	173	OD	yes	yes	5.67	61	51	54	51	88
				OS	yes	yes	6.11	61	49	64	53	77
P4	m	39	50	OD	yes	no	5.70	60	53	78	49	59
				OS	yes	yes	6.63	82	63	95	60	111
P5	f	22	41	OD	yes	yes	6.26	67	65	58	64	83
				OS	yes	yes	6.21	73	67	69	67	89
P6	f	30	128	OD	no	no	6.61	88	76	84	71	121
				OS	no	no	6.64	93	70	125	64	115
P7	f	20	66	OD	yes	yes	6.52	96	74	103	74	131
				OS	yes	yes	6.86	115	72	132	107	149
P8	f	45	69	OD	yes	yes	5.25	62	52	70	41	83
				OS	yes	yes	5.55	52	57	56	31	65
P9	f	47	3	OD	yes	yes	6.66	86	74	103	63	103
				OS	yes	yes	6.57	79	69	99	56	93

Abbreviations: Pat. = Patient No; Age = age of onset; Dur. = time since diagnosis at time of OCT measurement in months; OD = right eye; OS = left eye; VS = visual symptoms; BRAO = branch retinal artery occlusion; TMV = total macular volume in mm^3; A = average retinal nerve fibre layer thickness (RNFLT) in μm; T = temporal, S = superior, N = nasal, I = inferior quadrant's RNFLT in μm.

doi:10.1371/journal.pone.0038741.t002

Study Design and Participants

This is a prospective, cross-sectional, multicentre observational study documenting OCT findings in Susac syndrome patients. Patients with definite diagnosis of Susac syndrome, aged ≥ 18 years were recruited from the neurologic outpatient clinics of five large university medical centres (Berlin, Münster, Düsseldorf, Hamburg, and Würzburg, Germany). Exclusion criteria were inability to provide informed consent. All included patients underwent complete neurological examination. Medical history, particularly with respect to encephalopathy, visual symptoms, and hearing loss was taken from all study participants. In cases where the classical clinical triad was not present, diagnosis was established on clinical presentation and MRI findings. Visual testing was performed with bedside visual field testing. Age and gender matched healthy controls (HC) and patients with relapsing remitting MS (RRMS) were randomly selected from the imaging research database of the NeuroCure Clinical Research Center (NCRC) at Charité – Universitätsmedizin Berlin by an investigator blinded to the OCT data.

Ethics

The study was approved by the local ethics committees and was conducted in accordance to the Declaration of Helsinki in its currently applicable version, the guidelines of the International Conference on Harmonisation of Good Clinical Practice (ICH-GCP), and the applicable German laws. All participants gave informed written consent.

Optical Coherence Tomography

RNFLT and TMV were measured with Stratus 3000 OCT (Carl Zeiss Meditec, California, USA) using "Fast RNFL 3.4" and "Fast Macula Thickness Map" protocols (software V4.0) by trained personnel. For RNFLT, a 3.4 mm diameter circular scan was acquired circumferentially to the optic disc, and for TMV six radial lines were taken, centred within the fovea. A good quality image was defined as having generalised signal distribution, a reflectance signal from either RNFL or retinal pigment epithelium strong enough to identify either layer, no missing parts caused by eye movements, and a signal strength of ≥7 of 10 [17]. Segmentation lines for upper and lower borders of RNFL were required to be on the internal limiting membrane and lower border of the RNFL. For the comparison of OCT measurements to normative data, the device's internal normative database, comprising of measurements of 170 eyes from HC was used as a reference. Percentile positions of measurements compared to these normative data are automatically given on the device's TMV and RNFLT report as below 1st percentile, between 1st and 5th percentile, between 5th and 95th percentile, and above 95th percentile.

Statistical methods

Differences in age and time since diagnosis between patients with Susac syndrome, HC and RRMS patients with and without a history of optic neuritis were analysed using Friedman's analysis for matched pairs. Differences between eyes from the groups were assessed using generalised estimating equation models (GEE) accounting for intra-patient/inter-eye dependencies. To further rule out possible age related effects or effects related to minor differences in time since diagnosis, GEE models were corrected for age and additionally with time since diagnosis for comparisons against RRMS patients. In all GEE, the diagnostic group was used as independent categorical variable. Mean values in text are given with standard deviation (SD) after a ± sign. All statistical tests were performed using SPSS 20 (IBM, Somers, NY, USA). For all calculations, statistical significance was established at $p<0.05$.

Results

Cohort description

Nine patients with Susac syndrome were prospectively recruited (six jointly from Berlin and Münster, one from each of the other

Table 3. Mean values from optical coherence tomography measurements of the macula (total macular volume and below) and the circular scan around the optic nerve head (RNFLT Average and below).

		Susac				HC				MS-NON				MS-ON			
		Mean	**SD**	**Min**	**Max**	**Mean**	**SD**	**Min**	**Max**	**Mean**	**SD**	**Min**	**Max**	**Mean**	**SD**	**Min**	**Max**
Total Macular Volume [mm³]		**6,43**	**0,67**	**5,25**	**7,66**	**7,14**	**0,35**	**6,65**	**7,84**	**7,09**	**0,36**	**6,51**	**7,75**	**6,73**	**0,49**	**6,04**	**7,68**
Inner Macula	**T [µm]**	240	33	172	284	269	18	238	296	269	13	237	286	253	20	220	294
	S [µm]	242	55	128	300	283	16	255	308	281	17	239	301	265	19	237	296
	N [µm]	271	26	207	306	282	17	256	312	279	16	243	302	266	19	241	302
	I [µm]	254	42	146	301	280	18	254	311	281	12	258	301	260	21	232	304
Outer Macula	**T [µm]**	205	27	160	243	229	11	213	252	229	11	211	251	219	18	193	252
	S [µm]	209	42	139	263	247	12	231	276	245	14	222	266	234	17	209	263
	N [µm]	246	18	211	267	264	14	248	291	262	16	232	291	248	18	214	281
	I [µm]	222	30	143	265	242	12	223	262	241	11	216	267	226	18	200	266
RNFLT Average [µm]		**81**	**18**	**52**	**115**	**107**	**9**	**91**	**120**	**102**	**14**	**87**	**137**	**95**	**11**	**74**	**118**
RNFLT	**T [µm]**	65	11	48	81	75	12	59	101	73	17	49	109	57	14	29	77
	S [µm]	93	28	54	141	133	14	104	158	123	17	104	164	113	16	87	150
	N [µm]	65	21	31	107	85	16	67	120	82	21	47	142	90	16	62	123
	I [µm]	101	24	59	149	132	14	109	150	128	17	105	163	120	16	89	139

Abbreviations: RRMS = relapsing-remitting multiple sclerosis; HC = healthy controls; SD = standard deviation; RNFLT = retinal nerve fibre layer thickness; t = temporal; S = superior; N = nasal; I = inferior.

doi:10.1371/journal.pone.0038741.t003

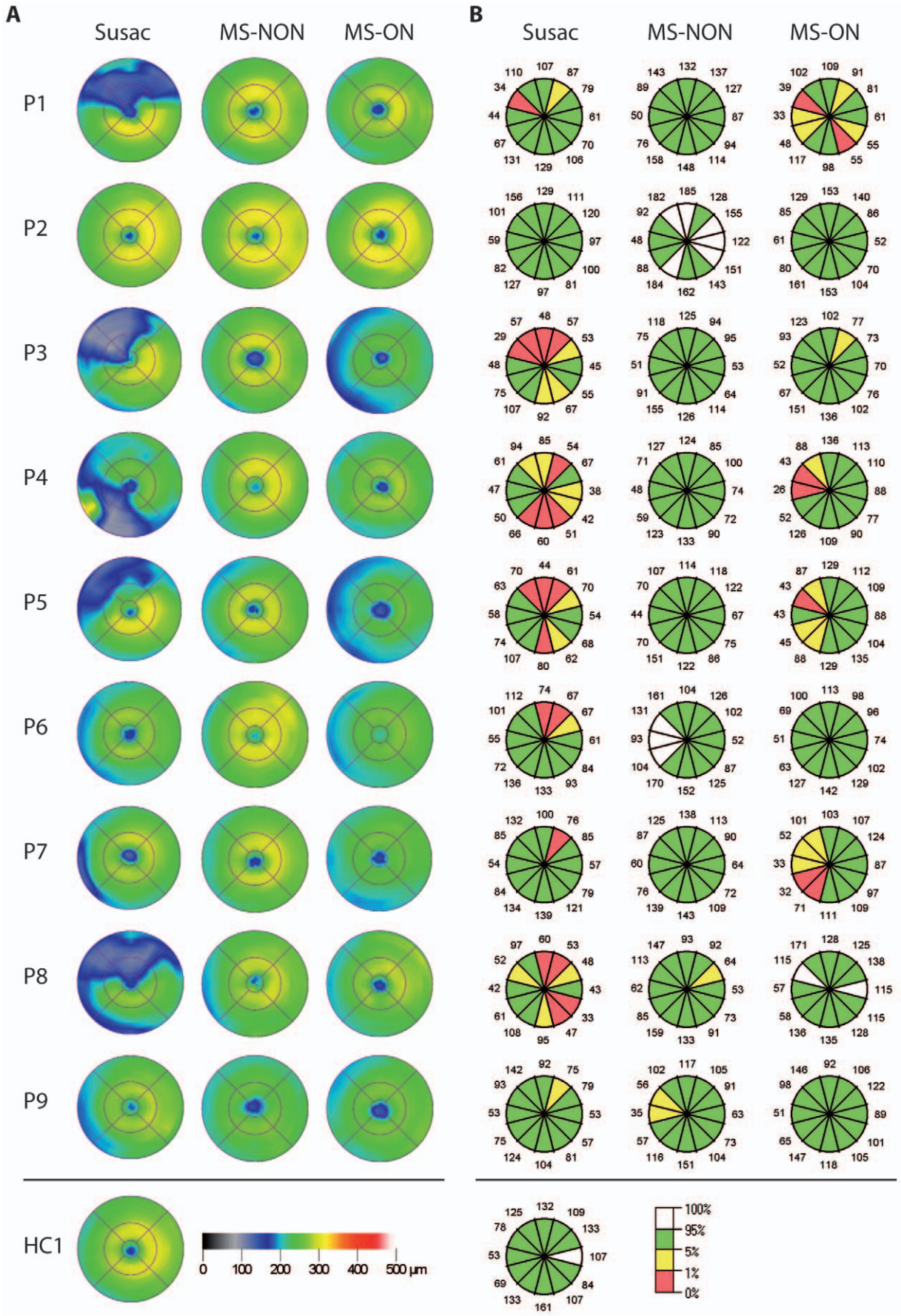
A
Susac
MS-NON
MS-ON
P1
P2
P3
P4
P5
P6
P7
P8
P9
HC1
0
100
200
300
400
500 µm
B
Susac
MS-NON
MS-ON
100%
95%
5%
1%
0%

Figure 1. Macular and ring scans from patients with Susac syndrome and matched RRMS patients. Shown are only the left eyes (randomly selected to save space) from each Susac patient (P1-9) and the corresponding left eyes from RRMS patients without history of optic neuritis (MS-NON) and RRMS patients with history of optic neuritis (MS-ON). On the bottom, a comparison of scans from one of the healthy controls is given. A) Colour coded is the calculated macular thickness from the device's segmentation algorithm with black to blue for reduced thickness and yellow to green for normal thickness (left legend on the bottom). The macular thickness map is calculated from six linear scans through the centre of the macula. Of note is the different distribution of the damage. B) For RNFLT scans, the thickness from 12 clock-hour segments of the circular scan is given. Colour coded is the thickness relative to the normative database with green and white meaning normal values above the 5th or 95th percentile and yellow and red meaning reduction of thickness below the 5th or 1st percentile (right legend on the bottom). Whereas some Susac patients' eyes show striking sectoral damage, eyes from RRMS patients show an even thinning with an accentuation in the outer temporal areas, that is further pronounced with a history of optic neuritis. Three Susac patients (P6, 7, 9) show a similar pattern.
doi:10.1371/journal.pone.0038741.g001

three centres). A demographic overview is given in table 1, and a multiple case presentation is provided in table 2. The female to male ratio of 2:1 reflected that reported in the literature. All patients had a history of hearing loss, and all but one patient (P2) had symptoms of encephalopathy. All patients except one (P6) had a history of visual symptoms and provided accompanying reports of BRAO. Additionally, one patient (P2) had visual symptoms on the right eye. However, in this patient a report of BRAO did exist for both eyes. At the time of OCT investigation, no patient was in a clinically active phase of the disease.

Macular and retinal nerve fibre layer damage

Single case OCT measurements are given in table 2, and a synopsis is provided in table 3. In summary, compared to the normative database of the OCT device, most patients showed a reduction in either average RNFLT or macular measurements. All but one patient (P2) with a history of visual symptoms showed either reduced average RNFLT and/or diminished TMV in at least one eye. P2 showed a very mild clinical phenotype and TMV was above the 95th percentile when compared to the normative database of the device. Interestingly, one patient without visual symptoms and without documented BRAO (P6) did also present a pathological OCT with a strong RNFLT reduction in the superior quadrant of the right eye, although average RNFLT in this eye was normal (figures 1 and 2).

Importantly, TMV and RNFLT reduction were not evenly distributed over the entire scanning area but scattered over all sectors (figure 1 and figure 2). Patients with Susac syndrome showed a RNFLT below the 5th percentile in a mean 3.6±3.4 (range 0–10) of the twelve clock-hour sectors and a TMV below the 5th percentile in a mean 2.4±2.9 (range 0–7) of the nine macular sectors whereas the other sectors were within normal ranges. All but one patient (P2) showed this patchy retinal damage in at least one eye as indicated by the yellow and red areas in the RNFLT measurements and the dark blue areas in the TMV measurements (figure 1).

Comparison to matched healthy controls and multiple sclerosis patients

To compare OCT results from patients with Susac syndrome to results from HC and RRMS patients, either group of nine gender and age matched HC (mean age 33±11 years, 3/6 male/female), nine RRMS patients without any history of optic neuritis (mean age 32±10 years, 3/6 male/female, time since diagnosis 55±40 months) and nine RRMS patient with a previous bilateral optic neuritis (mean age 33±9 years, 3/6 male female, time since diagnosis 38±40 months) was considered. HC and RRMS patients were matched for gender, age and time since diagnosis. Gender was matched exactly 1:1. The differences in age were not significant (Friedman's analysis for matched pairs $p = 0.661$). Likewise, time since diagnosis of RRMS patients with and without previous optic neuritis was statistically not different from Susac patients (Friedman's analysis for matched pairs $p = 0.062$).

Average RNFLT was reduced in patients with Susac syndrome (average RNFLT 81±18 µm, table 3) in comparison to HC (average RNFLT 107±9 µm, coefficient $B = -25.5$, SE 6.2, $p<0.001$, GEE), RRMS patients without previous optic neuritis (average RNFLT 102±14 µm, coefficient $B = -21.3$, SE 6.2, $p = 0.001$, GEE) and RRMS patients with a history of optic neuritis (average RNFLT 95±11 µm, coefficient $B = -13.5$, SE 5.8, $p = 0.019$, GEE) (figure 1B, 2 and 3). Accordingly, TMV was reduced in patients with Susac syndrome (TMV 6.43±0.67 mm^3, table 3) in comparison to HC (TMV 7.14±0.35 mm^3, coefficient $B = -0.71$, SE 0.22, $p = 0.001$, GEE), RRMS patients without history of optic neuritis (TMV 7.09±0.36 mm^3, coefficient $B = -0.67$, SE 0.20, $p = 0.001$, GEE) but not against RRMS patients with previous history of optic neuritis (TMV 6.73±0.49 mm^3, coefficient $B = -0.23$, SE 0.21, $p = 0.224$, GEE) (figure 1 and 3).

Discussion

In this cross-sectional, observational study we investigated nine patients with Susac syndrome using OCT and compared RNFLT and TMV data with nine gender and age matched HC and nine RRMS patients each with or without history of optic neuritis. Our main findings are (a) pathologic OCT measurements in most of the Susac patients with a history of visual symptoms when compared to the normative database of the OCT device; (b) reduced RNFLT and macular measurements when compared to gender and age matched HC; (c) a more severe retinal nerve fibre damage in patients with Susac syndrome as compared to RRMS patients irrespective the history of optic neuritis despite a similar disease duration, and most importantly (d) distinct patterns of retinal or retinal nerve fibre layer damage among patients with Susac syndrome compared to RRMS patients that can help to discriminate between both diseases.

Although a rare disease, Susac syndrome needs to be considered in the differential diagnosis of a variety of neurological disorders. Currently, its diagnosis is based primarily on the clinical presentation, the documentation of BRAO by FAG, and characteristic findings on cranial magnetic resonance imaging, including subtle changes such as fibre impairment detected by diffusion tensor imaging [18]. Recently, anti-endothelial antibodies in Susac syndrome were reported as a potential future diagnostic criterion and as a possible pathologic correlate [19,20].

The majority of patients with Susac syndrome in this study showed a characteristic and thus very distinct pattern of often severe and patchy retinal nerve fibre thinning in RNFLT and retinal damage in TMV. Compatible with the pathology of this retinal microangiopathy, retinal damage was usually scattered over distinct foci and not evenly distributed: whereas several sectors in RNFLT and/or TMV showed severe damage, other sectors remained completely normal. The notable exclusion from that rule was patient P2, who had a mostly normal RNFLT and TMV, despite visual symptoms and BRAO findings in FAG.

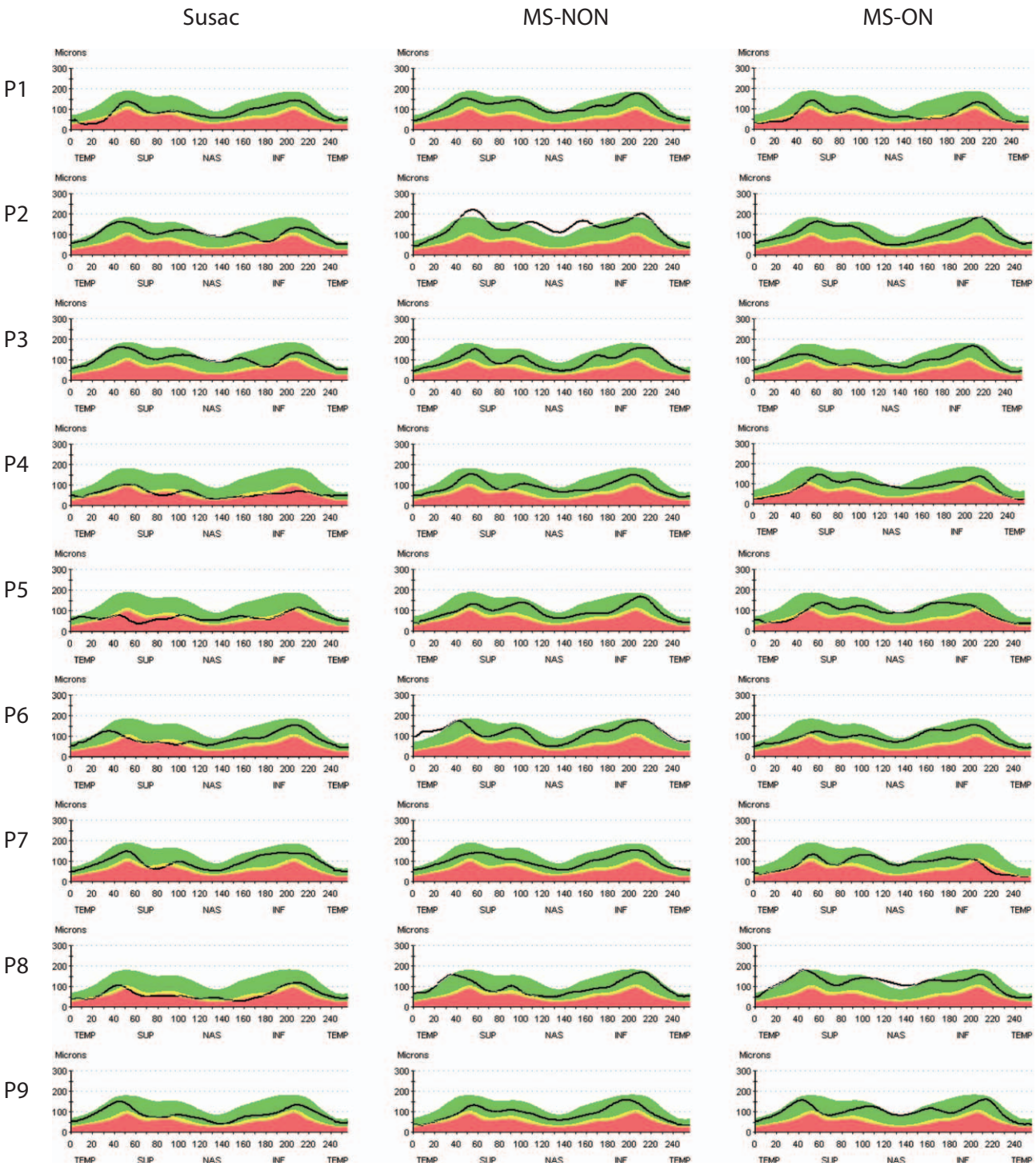

Figure 2. RNFLT from patients with Susac syndrome and matched RRMS patients. Shown are only the left eyes (randomly selected to save space) from each Susac patient (P1-9) and the corresponding left eyes from RRMS patients without history of optic neuritis (MS-NON) and RRMS patients with history of optic neuritis (MS-ON). Each graph represents the RNFLT from a peripapillary ring scan. Colour coded is the thickness relative to the normative database with green and white meaning normal values above the 5th or 95th percentile and yellow and red meaning reduction of thickness below the 5th or 1st percentile. Abbreviations: RNFLT = retinal nerve fibre layer thickness.
doi:10.1371/journal.pone.0038741.g002

This presentation of Susac syndrome in OCT is in contrast to OCT findings in MS. Several publications that were recently reviewed in a meta-analysis [16], report an evenly distributed thinning of RNFL in MS that is slightly enhanced on the temporal quadrant after optic neuritis [21]. However, RNFL thinning in MS accumulates over time and becomes more severe especially in later stages of the disease. In early stages of MS and in clinically isolated syndrome (CIS), when differentiation of Susac syndrome is most important, RNFL thinning is barely detectable [22]. However, since Susac patients in this study's cohort had an

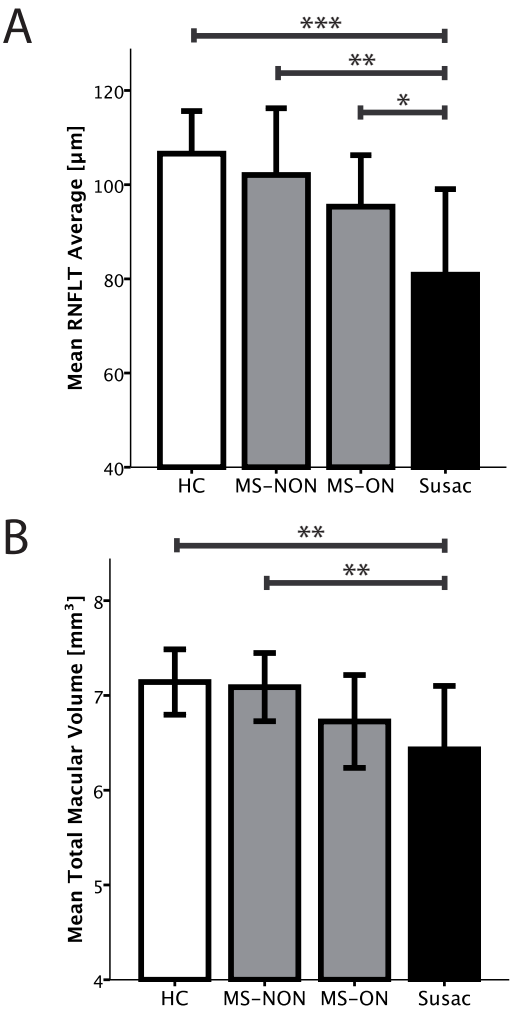

Figure 3. Comparison between healthy controls, RRMS patients and patients with Susac syndrome. Error bars indicate 1-fold standard deviation. Significance level from Generalised Estimating Equations are given as ***) $p<0.001$, **) $p<0.01$, and *) $p<0.05$. *Abbreviations*: HC = healthy control; RRMS = relapsing remitting multiple sclerosis; RNFLT = retinal nerve fibre layer thickness; MS-ON = RRMS patients with a previous, bilateral optic neuritis; MS-NON = RRMS patients without a history of optic neuritis.
doi:10.1371/journal.pone.0038741.g003

established diagnosis already for several months or even years, it is not clear, how early Susac syndrome with acute visual impairment and BRAO translate into pathological OCT findings.

The crucial question in this context is at what time point OCT starts to show abnormal findings in patients with Susac syndrome. A few case reports and one study with nine BRAO patients without underlying Susac syndrome report an initial thickening of RNFL leading to final thinning after several months [23–25]. In general, one would suspect that structural retinal nerve fibre damage evolves some time after the underlying vessel pathology. One patient (P6) however showed an abnormal OCT even without BRAO in FAG pointing towards a potential usability of OCT in earlier stages of the disease when the diagnosis is yet not fully established. This issue should be addressed in a longitudinal study investigating the development of retinal lesions of newly diagnosed patients with Susac syndrome and BRAO over time including functional visual outcomes. Due to the design of our study, it was not possible to perform FAG and OCT at the same time, unfortunately limiting the possibility to make assertions on the co-occurrence of OCT and BRAO findings in this respect. Therefore, these questions are currently investigated in a follow up study.

Beyond differential diagnosis, the severe structural retinal damage in Susac syndrome especially in the macular scans detected by OCT supports an aggressive treatment regimen early after diagnosis [8]. This notion is further assisted by the fact that patient (P6) without visual symptoms showed a pathological OCT, suggesting early subclinical retinal damage. On the other hand, one patient (P2) with actual BRAO did not have pathological findings in OCT. Thus, BRAO does not always lead to pathological OCT findings. The dissociation of retinal damage and history of BRAO observed in P2 and P6 might suggest additional mechanisms independent of BRAO underlying retinal damage in this disease.

The reported study has important limitations that need to be considered. Due to the rarity of the disease, recruitment of a sufficient number of patients is challenging and prospective data on Susac syndrome derived from studies with more than five patients hardly exist. Although data on a limited number of nine patients obviously need to be interpreted cautiously, our study is among the largest prospective studies so far reported on Susac syndrome [26–28]. However, conclusions on the discriminatory ability of OCT between Susac syndrome and MS should be interpreted with care from this study with only small numbers.

Another important limitation of our study is the use of a time domain OCT device that measures macular volume using a six-line scan protocol instead of a volume/3D scan. A thickness map is generated via interpolating the measurements between the six line scans. The distinct and striking sectorial damage in the macular scans might therefore be under- or overestimated. Since the macular scan incorporates all retinal layers between the inner limiting membrane and the retinal pigment epithelium, it is not possible to determine via time domain OCT alone, which retinal layers are affected in Susac syndrome in comparison to optic neuritis. Because of the vascular nature of the disease, one might speculate though, that any damage would be more profound and affecting more retinal layers when compared to optic neuritis. Furthermore, the used time domain OCT device has known limitations in the reproducibility of sectoral RNFLT [29]. Next generation spectral domain OCT devices provide volume 3D scans and intra-retinal segmentation algorithms [30], possibly further enhancing the value of OCT in the differential diagnosis of Susac syndrome. However, in contrast to spectral domain OCT, time domain OCT is already widely available and patients with Susac syndrome show the reported distinct phenotype in comparison to MS even in time domain OCT, thus strengthening the importance of OCT application in differential diagnosis in routine or outpatient clinic settings.

In summary, we show that Susac patients regularly have distinct abnormalities in OCT scans. The sectorial pattern of retinal damage supports the hypothesis of a vascular origin with patchy lesions. Most importantly, our data recommends OCT as a tool in early primary and secondary diagnostics of Susac syndrome when differentiation from MS and other neuroimmunologic diseases can prove challenging.

Acknowledgments

We thank our study nurses Franziska Lipske and Katja Wolf for important logistical support.

Author Contributions

Conceived and designed the experiments: JD IK FP AUB. Performed the experiments: HZ FK JP SS DF MR OA CG IK JD. Analyzed the data: JD AUB FP. Wrote the paper: AUB IK JD. Provided important intellectual input into design and conduct of study: OA EBR HPH FP. Provided crucial logistic support: EBR CG OA MR HPH. Critically revised the manuscript for intellectual content: HZ FK JP SS DF OA CG MR EBR HPH FP.

References

1. Susac JO, Hardman JM, Selhorst JB (1979) Microangiopathy of the brain and retina. Neurology 29: 313–316.
2. Susac JO (1994) Susac's syndrome: the triad of microangiopathy of the brain and retina with hearing loss in young women. Neurology 44: 591–593.
3. Dörr J, Radbruch H, Bock M, Wuerfel J, Brüggemann A, et al. (2009) Encephalopathy, visual disturbance and hearing loss-recognizing the symptoms of Susac syndrome. Nat Rev Neurol 5: 683–688.
4. Petty GW, Engel AG, Younge BR, Duffy J, Yanagihara T, et al. (1998) Retinocochleocerebral vasculopathy. Medicine (Baltimore) 77: 12–40.
5. McLeod DS, Ying HS, McLeod CA, Grebe R, Lubow M, et al. (2011) Retinal and optic nerve head pathology in Susac's syndrome. Ophthalmology 118: 548–552.
6. Susac JO, Egan RA, Rennebohm RM, Lubow M (2007) Susac's syndrome: 1975–2005 microangiopathy/autoimmune endotheliopathy. J Neurol Sci 257: 270–272.
7. Petty GW, Matteson EL, Younge BR, McDonald TJ, Wood CP (2001) Recurrence of Susac syndrome (retinocochleocerebral vasculopathy) after remission of 18 years. Mayo Clin Proc 76: 958–960.
8. Rennebohm RM, Egan RA, Susac JO (2008) Treatment of Susac's Syndrome. Curr Treat Options Neurol 10: 67–74.
9. Rennebohm RM, Susac JO (2007) Treatment of Susac's syndrome. J Neurol Sci 257: 215–220.
10. Egan RA, Hills WL, Susac JO (2010) Gass plaques and fluorescein leakage in Susac Syndrome. J Neurol Sci 299: 97–100.
11. Rennebohm R, Susac JO, Egan RA, Daroff RB (2010) Susac's Syndrome – update. J Neurol Sci 299: 86–91.
12. O'Halloran HS, Pearson PA, Lee WB, Susac JO, Berger JR (1998) Microangiopathy of the brain, retina, and cochlea (Susac syndrome). A report of five cases and a review of the literature. Ophthalmology 105: 1038–1044.
13. Frohman EM, Costello F, Zivadinov R, Stuve O, Conger A, et al. (2006) Optical coherence tomography in multiple sclerosis. Lancet Neurol 5: 853–863.
14. Frohman EM, Fujimoto JG, Frohman TC, Calabresi PA, Cutter G, et al. (2008) Optical coherence tomography: a window into the mechanisms of multiple sclerosis. Nature Clinical Practice Neurology 4: 664–675.
15. Naismith RT, Tutlam NT, Xu J, Klawiter EC, Shepherd J, et al. (2009) Optical coherence tomography differs in neuromyelitis optica compared with multiple sclerosis. Neurology 72: 1077–1082.
16. Petzold A, de Boer JF, Schippling S, Vermersch P, Kardon R, et al. (2010) Optical coherence tomography in multiple sclerosis: a systematic review and meta-analysis. Lancet Neurol 9: 921–932.
17. Cheung CYL, Leung CKS, Lin D, Pang C-P, Lam DSC (2008) Relationship between retinal nerve fiber layer measurement and signal strength in optical coherence tomography. Ophthalmology 115: 1347–51, 1351.e1–2.
18. Kleffner I, Deppe M, Mohammadi S, Schiffbauer H, Stupp N, et al. (2008) Diffusion tensor imaging demonstrates fiber impairment in Susac syndrome. Neurology 70: 1867–1869.
19. Jarius S, Neumayer B, Wandinger KP, Hartmann M, Wildemann B (2009) Anti-endothelial serum antibodies in a patient with Susac's syndrome. J Neurol Sci 285: 259–261.
20. Magro CM, Poe JC, Lubow M, Susac JO (2011) Susac syndrome: an organ-specific autoimmune endotheliopathy syndrome associated with anti-endothelial cell antibodies. Am J Clin Pathol 136: 903–912.
21. Bock M, Brandt AU, Dörr J, Kraft H, Weinges-Evers N, et al. (2010) Patterns of retinal nerve fiber layer loss in multiple sclerosis patients with or without optic neuritis and glaucoma patients. Clin Neurol Neurosurg 112: 647–652.
22. Outteryck O, Zephir H, Defoort S, Bouyon M, Debruyne P, et al. (2009) Optical coherence tomography in clinically isolated syndrome: no evidence of subclinical retinal axonal loss. Arch Neurol 66: 1373–1377.
23. Asefzadeh B, Ninyo K (2008) Longitudinal analysis of retinal changes after branch retinal artery occlusion using optical coherence tomography. Optometry 79: 85–89.
24. Takahashi H, Iijima H (2009) Sectoral thinning of the retina after branch retinal artery occlusion. Jpn J Ophthalmol 53: 494–500.
25. Shah VA, Wallace B, Sabates NR (2010) Spectral domain optical coherence tomography findings of acute branch retinal artery occlusion from calcific embolus. Indian J Ophthalmol 58: 523–524.
26. Susac JO, Murtagh FR, Egan RA, Berger JR, Bakshi R, et al. (2003) MRI findings in Susac's syndrome. Neurology 61: 1783–1787.
27. Aubart-Cohen F, Klein I, Alexandra J-F, Bodaghi B, Doan S, et al. (2007) Long-term outcome in Susac syndrome. Medicine (Baltimore) 86: 93–102.
28. Kleffner I, Deppe M, Mohammadi S, Schwindt W, Sommer J, et al. (2010) Neuroimaging in Susac's syndrome: focus on DTI. J Neurol Sci 299: 92–96.
29. Cettomai D, Pulicken M, Gordon-Lipkin E, Salter A, Frohman TC, et al. (2008) Reproducibility of optical coherence tomography in multiple sclerosis. Arch Neurol 65: 1218–1222.
30. Saidha S, Syc SB, Ibrahim MA, Eckstein C, Warner CV, et al. (2011) Primary retinal pathology in multiple sclerosis as detected by optical coherence tomography. Brain 134: 518–533.

Hindawi Publishing Corporation
Multiple Sclerosis International
Volume 2012, Article ID 530305, 10 pages
doi:10.1155/2012/530305

Clinical Study

Retinal Damage in Multiple Sclerosis Disease Subtypes Measured by High-Resolution Optical Coherence Tomography

Timm Oberwahrenbrock,[1] Sven Schippling,[2,3] Marius Ringelstein,[4] Falko Kaufhold,[1] Hanna Zimmermann,[1] Nazmiye Keser,[4] Kim Lea Young,[2] Jens Harmel,[4] Hans-Peter Hartung,[4] Roland Martin,[2,3] Friedemann Paul,[1,5] Orhan Aktas,[4] and Alexander U. Brandt[1]

[1] *NeuroCure Clinical Research Center and Experimental and Clinical Research Center, Charité University Medicine Berlin/Max Delbrück Center for Molecular Medicine, 10117 Berlin, Germany*
[2] *Institute for Neuroimmunology and Clinical Multiple Sclerosis Research (inims), University Medical Center Hamburg-Eppendorf, 20251 Hamburg, Germany*
[3] *Department of Neuroimmunology and Clinical Multiple Sclerosis Research, Neurology Clinic, University Hospital Zurich, 8091 Zurich, Switzerland*
[4] *Department of Neurology, Medical Faculty, Heinrich-Heine-University Düsseldorf, 40225 Düsseldorf, Germany*
[5] *Clinical and Experimental Multiple Sclerosis Research Center, Charité University Medicine Berlin, 10117 Berlin, Germany*

Correspondence should be addressed to Friedemann Paul, friedemann.paul@charite.de

Received 24 February 2012; Revised 8 May 2012; Accepted 18 May 2012

Academic Editor: Mark S. Freedman

Background. Optical coherence tomography (OCT) has facilitated characterisation of retinal alterations in MS patients. Only scarce and in part conflicting data exists on different MS subtypes. *Objective.* To analyse patterns of retinal changes in different subtypes of MS with latest spectral-domain technology. *Methods.* In a three-centre cross-sectional study 414 MS patients and 94 healthy controls underwent spectral-domain OCT examination. *Results.* Eyes of MS patients without a previous optic neuritis showed a significant reduction of both retinal nerve fibre layer (RNFL) thickness and total macular volume (TMV) compared to healthy controls independent of the MS subtype ($P < 0.001$ for all subtypes). RNFL thickness was lower in secondary progressive MS (SPMS) eyes compared to relapsing-remitting MS (RRMS) eyes ($P = 0.007$), and TMV was reduced in SPMS and primary progressive MS (PPMS) eyes compared to RRMS eyes (SPMS: $P = 0.039$, PPMS: $P = 0.005$). Independent of the subtype a more pronounced RNFL thinning and TMV reduction were found in eyes with a previous optic neuritis compared to unaffected eyes. *Conclusion.* Analysis of this large-scale cross-sectional dataset of MS patients studied with spectral-domain OCT confirmed and allows to generalize previous findings. Furthermore it carves out distinct patterns in different MS subtypes.

1. Introduction

Multiple sclerosis is an inflammatory and neurodegenerative disorder of the central nervous system that leads to a progressive axonal loss and degeneration of neurons. Whereas a vast majority of MS patients present with a relapsing-remitting disease course (RRMS) that may subsequently transforms into secondary progressive MS (SPMS), a smaller portion of patients shows a progressive course (PPMS) from the very beginning of the disease [1].

Optical coherence tomography (OCT) is an increasingly recognized, noninvasive tool in MS imaging that allows cost-effective investigation of the retina [2] in a disease in which pathology of the anterior visual system is common. Over the recent past, OCT has emerged as a potential marker of axonal retinal degeneration in MS patients [3]. Of note, an increasing number of studies have consistently shown an association between OCT measures of retinal atrophy and markers of degeneration derived from either structural magnetic resonance imaging or MR spectroscopy (MRS) studies

[4–11] and between OCT measures and functional visual parameters as well as physical disability and cognitive performance [12–17]. Retinal nerve fibre layer (RNFL) thickness and total macular volume (TMV) are the most frequently investigated OCT parameters. They provide a unique opportunity to quantify the integrity of nonmyelinated axonal tissue (RNFL) as well as all retinal layers (TMV), including cellular segments, by a noninvasive imaging technique. RNFL and TMV reduction can be detected in eyes with (MS-ON) or without a previous history of optic neuritis (MS-NON) applying different OCT devices [15, 18–29]. Data on distinct differences in OCT findings between MS subtypes are scarce, and the results are at least in part conflicting. In general, cross-sectional studies show a more profound thinning of RNFL in progressive forms of MS compared to RRMS patients. However, it remains unresolved to date whether these differences are a genuine effect of the disease subtype *per se* or rather a function of disease duration, the number of optic neuritis (ON) episodes in the patients' history, or disease severity [30–34].

Most OCT studies previously performed in MS applied time-domain technology. Only very recently spectral-domain technology became available which enables imaging at substantially higher resolution without an increase in scanning time [16, 22, 34–38]. Here we report results from the largest multicentre cohort of MS patients and healthy controls (HC) thus far, studied in three dedicated MS centres in Germany, applying latest high-resolution spectral-domain OCT (SD-OCT) technology. In this large cohort, we reliably identified patterns of RNFL thinning and TMV reduction among different MS subtypes both with and without a history of ON when controlling for disease duration and severity, age, and gender.

2. Materials and Methods

2.1. Patients and Controls. 414 patients and 94 healthy controls were recruited in three dedicated MS units in the respective outpatient clinics at the Charité University Medicine Berlin (NeuroCure Clinical Research Center (NCRC)), at the Department of Neurology of the Heinrich-Heine University Düsseldorf (UKD) and in Hamburg (Institute for Neuroimmunology and Clinical MS Research (inims)). Data from a subgroup has previously been reported in Brandt et al. [23]. Inclusion criteria were age between 18 and 60 years and a definite diagnosis of MS according to the revised 2005 McDonald criteria [39]. MS subtype classification in RRMS, SPMS, or PPMS was based on the clinical course as assessed by the treating physician using Lublin criteria [40]. A history of ON had to be clearly determinable either by existing medical records, a VEP suggestive of optic neuritis, or by patient self-reports. Only eyes in which a history of ON could either be confirmed by clinical records or ruled out were subsequently included in the analysis. Patients with a refractive error of ≥ 5.0 diopters or with a history of eye disease that may impact significantly on OCT measures (e.g., glaucoma, retinal disease, retinal surgery, and diabetes) were excluded. Other exclusion criteria were acute optic neuritis or any other acute relapse or steroid treatment less than six months prior to OCT assessment as well as any other neurological disease with possible ocular manifestations. Disease duration was calculated as time since diagnosis in months.

Participants were assessed in a clinical examination under supervision of board certified neurologists within 6 months of OCT. Extended disability status scale (EDSS) was calculated according to the current guidelines [41]. Time since diagnosis was determined by reviewing patients' medical records. Healthy control participants were recruited from the medical staff, patients' relatives, and other volunteers.

A total of 937 eyes (754 MS eyes and 183 HC eyes) were finally included, 79 eyes were excluded from the analysis either due to poor scan quality or incomplete clinical data, in detail missing data on history of ON.

2.2. Ethics. The study protocol was approved by the local ethics committee and was conducted in accordance with the Declaration of Helsinki (1964) in its currently applicable version, the Guidelines of the International Conference on Harmonization of Good Clinical Practice (ICH-GCP) and applicable German laws. All participants gave written informed consent.

2.3. Optical Coherence Tomography. Participants underwent SD-OCT examination using the Heidelberg Engineering Spectralis SD-OCT (Heidelberg Engineering, Heidelberg, Germany). For both eyes of each participant, RNFL thickness around the optic disc was acquired using the 3.4 mm circle scan with the eye tracker system (TrueTrack) activated and the maximum number of averaging frames in ART-MEAN mode were tried to achieve. For assessing the macular volume two different scan protocols were used: the system built-in macula scan (25 B-scans, scanning angle = $15^\circ \times 15^\circ$, ART = 9) was performed at the Hamburg and Düsseldorf sites, while for the macular volume determination at the NCRC a custom protocol (61 B-scans, scanning angle = $30^\circ \times 25^\circ$, ART = 13) was used. Irrespective of the macular scan type, the TMV was calculated using the device's software. All scans were performed by trained operators and were reviewed for sufficient signal strength, correct centring, and beam placement as well as segmentation. Only eyes that passed the quality review were included in the subsequent analysis.

2.4. Statistical Analysis. Group comparisons of demographic factors were analysed using Mann-Whitney U test (for age and EDSS) and Pearson's Chi-square test (for gender, alpha = 0.05). Within the MS cohort Spearman's Rho analysis was used for correlation of EDSS and disease duration.

Generalized estimation equation (GEE) models accounting for within-subject intereye correlations were applied to test for differences of RNFL thickness and TMV between the study cohorts. GEE models were corrected for age and gender for the comparison of MS patients with HC and additionally for disease duration for MS subtype analysis. Associations of OCT with EDSS and regression analysis of disease duration with RNFL thickness and TMV were investigated with GEE models in a similar fashion. In all GEE

Table 1: Demographic and clinical data of multiple sclerosis patients (MS) and healthy controls (HC). MS patients are subdivided in the subtypes relapsing-remitting MS (RRMS), secondary-progressive MS (SPMS), and primary-progressive MS (PPMS).

		HC	MS			
			RRMS	SPMS	PPMS	All MS
No. of Subjects	Total	94	308	65	41	414
	Berlin	63	95	22	8	125
	Hamburg	0	158	23	22	203
	Düsseldorf	31	55	20	11	86
No. of Eyes (eyes with ON)	Total	183	561 (156)	116 (27)	77 (0)	754 (183)
	Berlin	122	187 (77)	44 (15)	16 (0)	247 (92)
	Hamburg	0	270 (54)	35 (2)	41 (0)	346 (56)
	Düsseldorf	61	104 (25)	37 (10)	20 (0)	161 (35)
Gender	Male (%)	31 (33)	87 (28)	29 (45)	24 (59)	140 (34)
	Female (%)	63 (67)	221 (72)	36 (55)	24 (41)	274 (66)
Age (in years)	Mean (SD)	34.47 (10.25)	39.10 (9.50)	48.23 (6.11)	46.90 (7.10)	41.31 (9.59)
	Range	19–56	19–58	33–59	32–59	19–59
Disease duration (in months)	Mean (SD)	NA	91.05 (80.26)	186.15 (87.94)	100.02 (93.33)	106.87 (89.51)
	Range	NA	0–384	39–403	4–426	0–426
EDSS	Median	NA	2.0	5.5	4.0	2.5
	Range	NA	0-7	3-8	2-8	0-8

models OCT measurements were included as the dependent variable. All statistical analyses were performed with R (R Version 2.12.2) including the *geepack* package for GEE models. Statistical significance was established at $P < 0.05$.

3. Results

3.1. Cohort Description. An overview of the demographic and basic clinical data including MS subtypes is given in Table 1. Healthy controls showed no significant gender differences to RRMS (Chi-square: $P = 0.452$) and SPMS (Chi-square: $P = 0.186$) patients, while gender composition of PPMS patients differed compared to HC (Chi-square: $P = 0.010$). Mean age of HC was significantly lower compared to all MS patients and all subtypes (Mann-Whitney U tests, $P < 0.001$ for all subtypes). RRMS patients were significantly younger than the progressive subtypes (Mann-Whitney U tests, $P < 0.001$ for SPMS and PPMS). As a consequence, age and gender were included as covariates in all GEE models. Time since diagnosis of RRMS and PPMS was significantly shorter compared to SPMS (Mann-Whitney U tests, $P < 0.001$ for both). Therefore, GEE models for MS subtype comparison were additionally adjusted for disease duration. Disease severity estimated by the EDSS was heterogeneous between MS subtypes as evaluated by Mann-Whitney U tests (RRMS versus SPMS: $P < 0.001$; RRMS versus PPMS: $P < 0.001$; SPMS versus PPMS: $P = 0.03$).

3.2. RNFL and TMV in MS-NON Eyes of Different MS Subtypes Compared to HC. For MS-NON eyes, differences in RNFL thickness and TMV compared to HC are given in Table 2. In summary, average peripapillary RNFL thickness was reduced in the pooled cohort of all MS patients' eyes and in all MS subtypes compared to HC (Figure 1(a)). Likewise, TMV was reduced for the pooled cohort of all MS patients' eyes and in all MS subtypes when compared to HC (Figure 1(b)). All alterations of RNFL and TMV in MS-NON eyes compared to control eyes showed strong statistical significance based on GEE models (Table 2). EDSS was inversely correlated with RNFL in case of all MS subtypes without a history of prior ON (RRMS-NON: $P = 0.007$; SPMS-NON: $P = 0.034$; PPMS-NON: $P = 0.006$). In contrast, the TMV was only significantly correlated with the EDSS in RRMS-NON eyes ($P = 0.003$), but not in SPMS-NON ($P = 0.321$) or PPMS-NON ($P = 0.085$).

3.3. Comparison of MS-ON Eyes with MS-NON Eyes and HC. Irrespective of the MS subtype, MS-ON eyes were significantly different from HC eyes for RNFL thickness and TMV (Figure 2) and showed a more pronounced RNFL thinning and TMV reduction when compared to MS-NON eyes (Table 3). RNFL thickness of RRMS-ON eyes and SPMS-ON eyes was significantly thinner compared to RRMS-NON or SPMS-NON eyes, respectively. The same was true for the TMV of ON-affected MS eyes, which was significantly reduced when compared to HC and to unaffected eyes of the same MS subtype (Table 3, Figure 2). The extent of RNFL thinning as well as TMV reduction was comparable between RRMS-ON and SPMS-ON eyes (RNFL GEE: $P = 0.369$; TMV GEE: $P = 0.124$). RRMS-ON eyes showed a significant inverse correlation between EDSS and RNFL ($P = 0.012$) while TMV did not reach significance ($P = 0.085$). For SPMS-ON eyes no significant correlation of EDSS with OCT parameters was found (RNFL: $P = 0.169$; TMV: $P = 0.573$).

3.4. Differences between Subtypes in MS-NON Eyes. Among MS subtypes, RRMS patients showed less RNFL thinning when compared to progressive subtypes (Table 2). When

Table 2: OCT results for the subtypes of MS patients without a history of optic neuritis (NON). Total retinal nerve fiber layer (RNFL) thickness (in μm) and total macular volume (TMV in mm^3) are given as mean values with standard deviation (SD). Generalized estimation equation (GEE) models were used to compare the MS cohorts to healthy controls. GEE models estimate the effect size with standard error (SE) and the respective P value.

			GEE models comparing MS OCT parameters to the healthy control cohort						
				RNFL thickness			TMV		
	Total RNFL thickness mean (SD) [μm]	TMV mean (SD) [mm^3]	Effect	Effect size	SE	P value	Effect size	SE	P value
MS-NON ($n = 571$)	90.15 (12.27)	8.48 (0.43)	Group	−9.571	1.177	<0.001	−0.235	0.043	<0.001
			Age	−0.132	0.053	0.013	−0.006	0.002	0.002
			Gender	2.272	1.116	0.042	−0.075	0.041	0.064
RRMS-NON ($n = 405$)	92.03 (11.91)	8.54 (0.42)	Group	−8.470	1.188	<0.001	−0.197	0.044	<0.001
			Age	−0.080	0.061	0.189	−0.003	0.002	0.094
			Gender	2.933	1.224	0.017	−0.107	0.045	0.019
SPMS-NON ($n = 89$)	83.14 (12.07)	8.32 (0.41)	Group	−9.951	1.084	<0.001	−0.248	0.039	<0.001
			Age	0.139	0.098	0.158	0.003	0.003	0.267
			Gender	−1.807	1.788	0.312	−0.150	0.062	0.015
PPMS-NON ($n = 77$)	88.35 (11.31)	8.34 (0.42)	Group	−4.253	0.792	<0.001	−0.141	0.027	<0.001
			Age	0.037	0.093	0.691	−0.001	0.003	0.654
			Gender	0.802	1.796	0.655	−0.044	0.064	0.492
HC ($n = 183$)	100.60 (9.41)	8.75 (0.34)	Group	N/A	N/A	N/A	N/A	N/A	N/A
			Age	N/A	N/A	N/A	N/A	N/A	N/A
			Gender	N/A	N/A	N/A	N/A	N/A	N/A

adjusting GEE models for age, gender, and disease duration, the only significant difference based on the mean total RNFL thickness was found between RRMS and SPMS patients, while patients with PPMS did not differ from either RRMS or SPMS (Table 4, Figure 1). As opposed to RNFL thickness a different pattern was obtained for TMV measures, in which a significant reduction was found for SPMS and PPMS when compared to RRMS patients. GEE models in which we additionally corrected for EDSS to account for different stages of disease severity did not show differences in RNFL thickness or TMV between MS subtypes (data not shown).

3.5. Association with Disease Duration and Yearly Atrophy Estimate. GEE models were used to test for an association of disease duration and RNFL thickness or TMV in MS eyes. MS-NON eyes showed an association of RNFL thickness and TMV with disease duration in the pooled cohort of all MS subtypes (Table 5, Figure 3). This association was retained in RRMS and SPMS eyes only for RNFL thickness and only in RRMS eyes for TMV. In all MS subtypes the correlation between RNFL thickness and TMV and disease duration was lost in ON eyes (data not shown).

Based on the effect size of the association of disease duration and RNFL thickness or TMV we estimated RNFL thinning and TMV reduction per year of ongoing disease in MS-NON eyes only (Table 5). RRMS-NON eyes showed the strongest and highly significant yearly changes for RNFL thickness (−0.495 μm/year) and TMV (−0.0155 mm^3/year). Interestingly, the significant yearly RNFL thinning in SPMS-NON eyes (−0.464 μm/year) was not concomitantly associated with a significant correlation in TMV change (−0.0016 mm^3/year, $P = 0.838$). In contrast, PPMS-NON eyes showed a less pronounced yearly RNFL thinning (−0.105 μm/year) but in relation a distinct reduction of TMV (−0.0111 mm^3/year). However, correlations of RNFL and TMV with disease duration were not significant for PPMS-NON eyes.

4. Discussion

Here we present the largest ever performed cross-sectional study on retinal atrophy measures in MS subtypes applying latest SD-OCT technology. Groups of disease subtypes in our study were sufficiently large to contrast findings in ON versus ON-free eyes within subgroups. Hereby we show that both RNFL and TMV are reduced in MS-NON eyes versus HC when pooling all disease subtypes, but also when separately comparing disease subtypes (RRMS, SPMS,

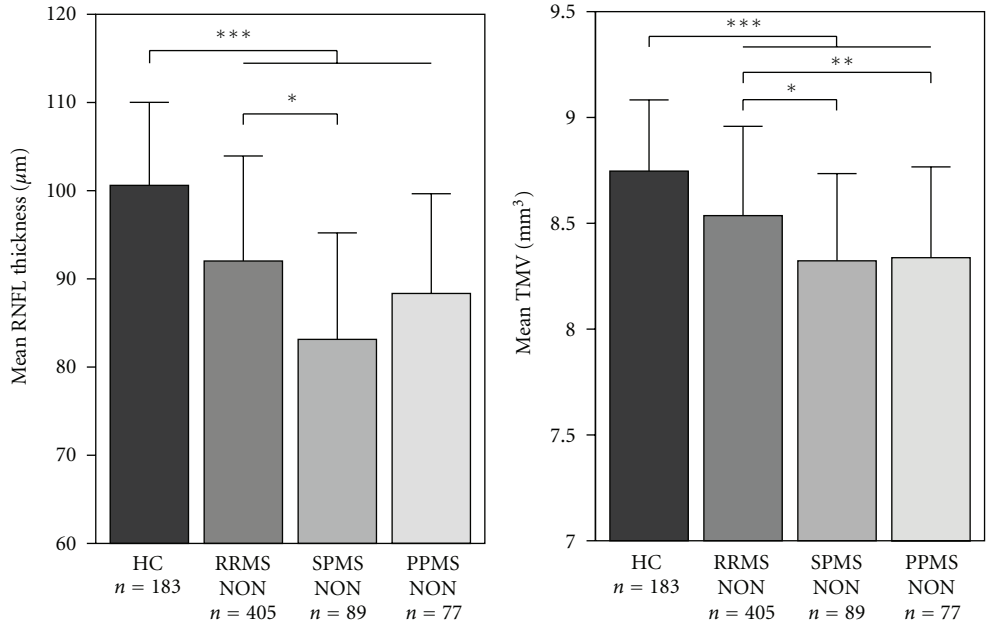

Figure 1: Mean retinal nerve fibre layer (RNFL) thickness (a) and mean total macular volume (TMV) (b) for the healthy controls (HC) and MS subtypes (RRMS, SPMS, and PPMS) without a history of optic neuritis (NON). Significant differences between the groups are indicated with $^{*}(P < 0.05)$, $^{**}(P < 0.01)$, and $^{***}(P < 0.001)$, respectively.

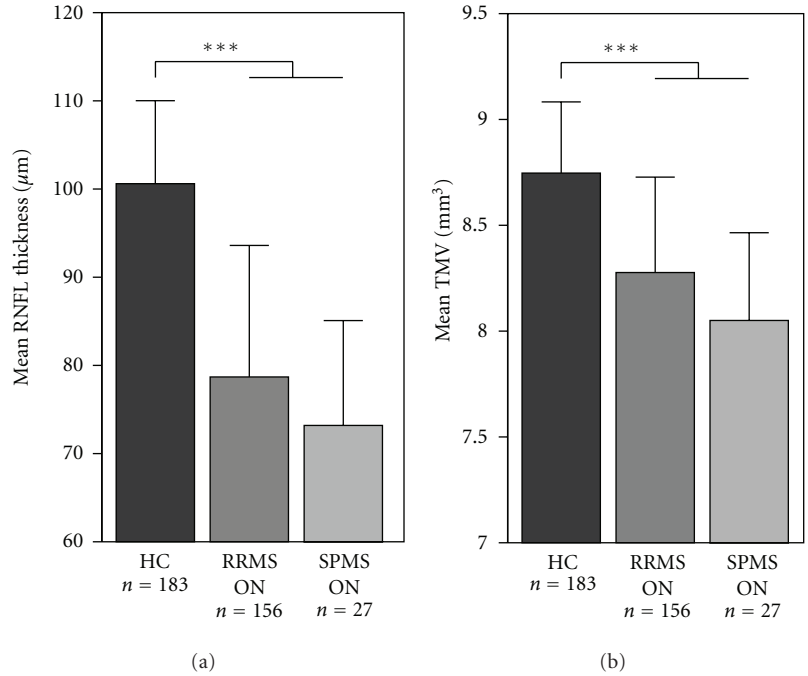

Figure 2: Mean retinal nerve fibre layer (RNFL) thickness (a) and mean total macular volume (TMV) (b) for the healthy controls (HC) and MS subtypes (RRMS, SPMS) with a history of optic neuritis (ON). Significant differences between the groups are indicated with $^{*}(P < 0.05)$, $^{**}(P < 0.01)$, and $^{***}(P < 0.001)$, respectively.

Table 3: OCT results for the subtypes of MS patients with a history of optic neuritis (ON). Total retinal nerve fiber layer (RNFL) thickness (in μm) and total macular volume (TMV in mm^3) are given as mean values with standard deviation (SD). ON eyes were compared to ON-non affected eyes of the same MS subtype using generalized estimation equation (GEE) models. GEE models estimate the effect size with standard error (SE) and the respective P value.

			GEE models comparing OCT parameters between ON-affected and unaffected eyes of the same subtype						
				RNFL thickness			TMV		
	Total RNFL thickness mean (SD) [μm]	TMV mean (SD) [mm^3]	Effect	Effect size	SE	P value	Effect size	SE	P value
MS-ON ($n = 183$)	77.88 (14.61)	8.24 (0.45)	Group	−12.199	1.336	<0.001	−0.237	0.043	<0.001
			Age	−0.147	0.056	0.008	−0.007	0.002	0.001
			Gender	2.989	1.161	0.010	−0.041	0.040	0.299
RRMS-ON ($n = 156$)	78.69 (14.91)	8.28 (0.45)	Group	−12.859	1.478	<0.001	−0.263	0.048	<0.001
			Age	−0.087	0.066	0.185	−0.004	0.002	0.071
			Gender	4.573	1.352	0.001	−0.048	0.046	0.295
SPMS-ON ($n = 27$)	73.19 (11.89)	8.05 (0.41)	Group	−9.297	2.802	0.001	−0.252	0.100	0.012
			Age	0.419	0.216	0.052	0.009	0.008	0.234
			Gender	−7.310	2.591	0.005	−0.250	0.091	0.006
PPMS-ON ($n = 0$)	N/A	N/A	N/A	N/A	N/A	N/A	N/A	N/A	N/A
HC ($n = 183$)	100.60 (9.41)	8.75 (0.34)	N/A	N/A	N/A	N/A	N/A	N/A	N/A

Table 4: Differences between MS subtypes without a history of optic neuritis (NON) were analyzed with generalized estimation equations (GEE) models including age, disease duration, and gender as effects.

	GEE models comparing OCT parameters between NON eyes of different MS subtypes						
		RNFL thickness			TMV		
	Effect	Effect size	SE	P value	Effect size	SE	P value
RRMS-NON versus SPMS-NON	Group	−5.144	1.921	0.007	−0.137	0.066	0.039
	Age	0.062	0.077	0.419	−0.001	0.003	0.775
	Duration	−0.044	0.009	<0.001	−0.001	0.0003	<0.001
	Gender	1.864	1.377	0.176	−0.139	0.051	0.007
RRMS-NON versus PPMS-NON	Group	−1.204	1.022	0.239	−0.104	0.037	0.005
	Age	−0.016	0.073	0.823	−0.002	0.003	0.371
	Duration	−0.034	0.008	<0.001	−0.001	0.0003	<0.001
	Gender	2.785	1.393	0.045	−0.102	0.052	0.051
SPMS-NON versus PPMS-NON	Group	2.634	2.494	0.291	−0.053	0.090	0.553
	Age	0.339	0.175	0.053	0.002	0.006	0.729
	Duration	−0.031	0.011	0.007	−0.001	0.0004	0.224
	Gender	−3.932	2.287	0.086	−0.127	0.086	0.139

and PPMS) to HC. Not surprisingly and in accordance with previous studies, MS-ON eyes exhibited more severe RNFL and TMV damage than MS-NON eyes. Both findings have been previously described in a similar way by various groups so that the nature of our study appears to be largely confirmatory at first glance. However, our study has some methodological advances compared to previous works that have important implications for the interpretation of our and previous OCT findings. The large sample size of our study enabled a statistically robust comparison of various disease subgroups with the inclusion of possible confounding factors such as age, disease duration, and gender in the statistical

Table 5: Generalized estimation equation (GEE) models correlating disease duration with RNFL thickness and TMV, respectively. The yearly change based on the effect sizes of the respective GEE model.

	RNFL thickness				TMV			
	Effect size	SE	*P* value	Change per year (μm)	Effect size	SE	*P* value	Change per year (mm^3)
All MS-NON	−0.0444	0.0068	<0.001	**−0.533**	−0.0012	0.0002	<0.001	**−0.014**
RRMS-NON	−0.0413	0.0088	<0.001	**−0.495**	−0.0013	0.0003	<0.001	**−0.016**
SPMS-NON	−0.0387	0.0174	0.026	**−0.464**	−0.0001	0.0006	0.838	**−0.002**
PPMS-NON	−0.0088	0.0151	0.562	**−0.105**	−0.0009	0.0006	0.131	**−0.011**

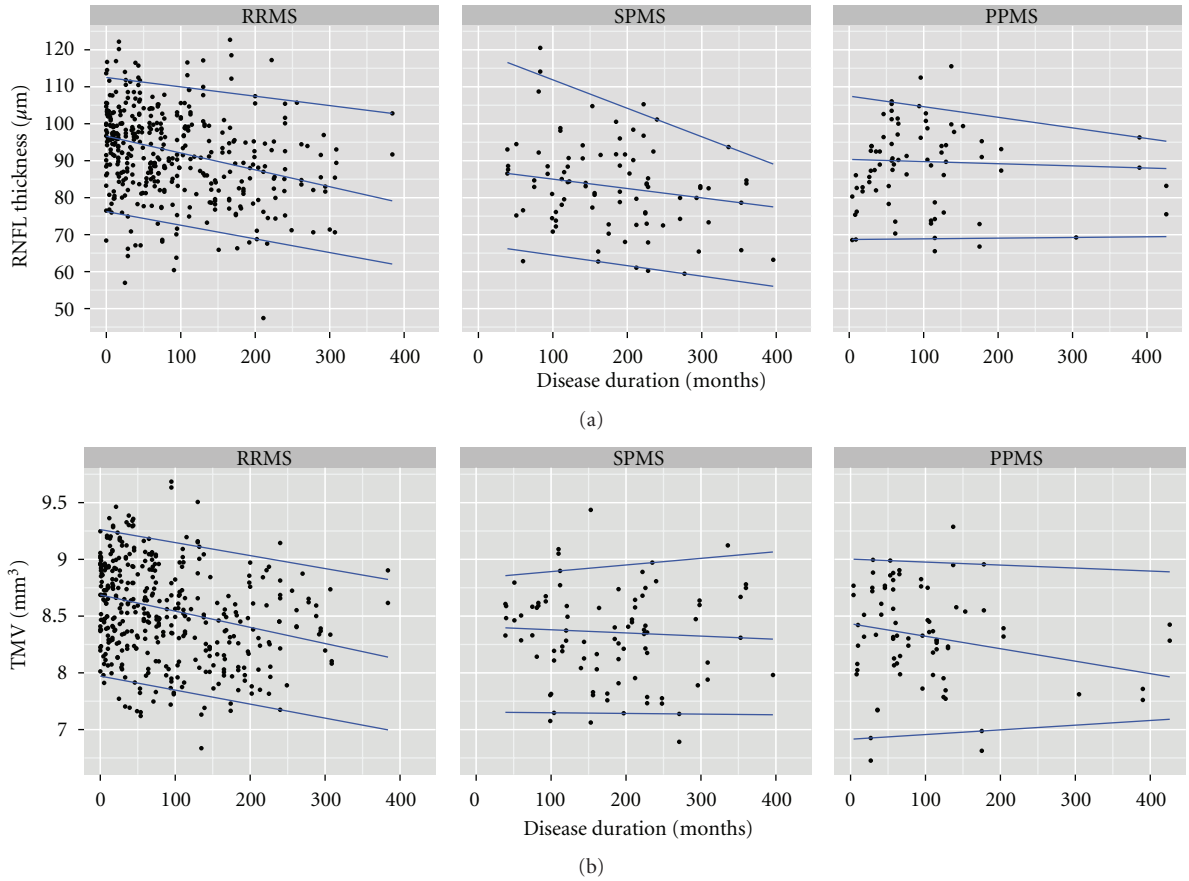

Figure 3: Association of RNFL thickness (a) and TMV (b) with disease duration for RRMS, SPMS and PPMS subtypes in eyes without previous optic neuritis. The blue lines indicate the 95%-, 50%- and 5%-quantiles.

models. In particular, we had larger numbers of patients in the progressive subgroups (65 SPMS, 41 PPMS) than any other previous study which allowed us to compare not only disease subtypes with HC but also with each other. This is of special interest against the background of the ongoing scientific debate on distinct pathogenetic mechanisms in, for example, PPMS versus RRMS. The subgroup comparisons revealed a significant reduction of RNFL thickness in SPMS patients versus RRMS after correction for age, gender, and disease duration and a significant reduction of TMV in both SPMS and PPMS patients versus RRMS.

In contrast, most previous works had only small sample sizes, especially for progressive subtypes which may—besides considerable differences in the statistical models—at least partly explain the inconsistent findings. Pulicken et al. (number of subjects: 135 RRMS, 16 SPMS, 12 PPMS, and 47 HC) found only trends towards lower RNFL thickness values in progressive disease versus RRMS and no difference in TMV in progressive MS versus RRMS [30]. Henderson et al. (number of subjects: 27 SPMS, 23 PPMS, and 20 HC) reported a significant reduction of RNFL and TMV versus HC only in NON eyes from SPMS patients but not PPMS patients and no difference between PPMS and SPMS [31]. Siepman et al. (number of subjects: 26 RRMS, 10 SPMS, and 29 PPMS) could not detect differences between PPMS-NON eyes and the pooled RRMS/SPMS-NON eyes [33].

Serbecic et al. (number of subjects: 42 RRMS, 17 SPMS, and 59 HC) did not specifically address differences in OCT measures between disease subtypes [34] as did numerous other studies with highly heterogeneous patient populations (Gordon-Lipkin et al. [6], number of subjects: 20 RRMS, 15 SPMS, 5 PPMS, and 15 HC; Toledo et al. [12], number of subjects: 7 CIS, 36 RRMS, 3 SPMS, 3 PPMS, 4 progressive-relapsing, and 18 HC; Fisher et al. [15], number of subjects: 90 MS, 76 of whom RRMS, and 36 HC; Sepulcre et al. [7], number of subjects: 22 CIS, 28 RRMS, 5 SPMS, 6 PPMS, and 29 HC), either because of insufficient subgroup sample sizes or owing to the fact that the study had goals other than comparing disease subtypes.

In line with several previous studies [16, 30, 31, 42, 43] we found higher RNFL measures in PPMS as compared to SPMS (88.4 μm versus 83.1 μm), which is in striking accordance with another study that also reported a difference of approximately 5 μm between PPMS and SPMS-NON eyes (93.9 μm versus 88.4 μm) [31]. Although these differences were not significant in both studies, these findings may point to a more severe RNFL damage in SPMS as compared to PPMS, which is in line with the clinical features of PPMS with a lower proportion of visual loss, less frequent ON attacks, a predominant clinical involvement of the spinal cord, and smaller brain lesions as compared to SPMS [31, 44, 45]. However, in contrast to Henderson et al. we found like in SPMS a significant reduction of TMV in NON eyes of PPMS patients versus RRMS and HC, which may display the neurodegenerative component of PPMS concomitantly reflected through brain atrophy measures [46].

Regarding the comparison of RNFL measures in RRMS and SPMS patients, we made another interesting observation: as described previously by Costello et al. [32], differences between SPMS-NON and RRMS-NON eyes were about twice that of differences between SPMS-ON and RRMS-ON eyes ($\sim$20 μm versus $\sim$10 μm in Costello's study, $\sim$10 μm versus $\sim$5 μm in our study). Costello et al. suggested that the impact of prior ON may outweigh the effects of disease subtype.

Further limitation of most of the previous studies is the utilization of time-domain OCT devices (TD-OCT) that only allow for 2-dimensional retinal imaging, limiting its use especially in the demanding macular investigations. The newer high-resolution spectral-domain OCT allows spatial imaging of the retina thus potentially greatly increasing the accuracy and value of OCT in MS [35, 36, 47]. First studies have already applied SD-OCT with intraretinal segmentation [16, 22, 26, 29]. Interestingly, the recent work by Saidha et al. supports the finding of a more severe neuroaxonal retinal damage in SPMS as compared to PPMS; a separate analysis of the combined ganglion cell layer and inner plexiform layer measured by Cirrus SD-OCT in different MS subtypes showed lowest values in SPMS [16]. In contrast, another study by Albrecht et al. [29] applying manual segmentation on Spectralis SD-OCT showed reduced measures in the deeper inner nuclear layer of PPMS but not SPMS patients versus HC. We presume that the ability of SD-OCT to measure spatial scans (earlier TD-OCT had to interpolate macular volume by using 6 radial linear scans) will in future greatly increase the value of macular scans over the currently preferred peripapillary ring scans. In addition, spatial scans allow for correction of positioning errors after scan acquisition by limiting the analysed area to a subset of the actual scan. For example, the Cirrus SD-OCT uses a spatial scan for the peripapillary ring scan, allowing for subsequent correction of alignment errors, whereas the Heidelberg Engineering Spectralis facilitates an eye tracker function to correct for eye movements. In TD-OCT, incorrect placement of peripapillary ring scans accounts to a significant extent for a weaker inter-measurement reliability and cannot be corrected after the scan has been acquired [48]. Next to the ability to analyse all intraretinal layers, improved test/retest-reliability distinguishes SD-OCT from TD-OCT and makes it an ideal instrument for the use in a longitudinal setting where inter-measurement reliability is crucial [49].

The time course of RNFL thinning and TMV reduction by atrophy of different retinal layers—be it in the context of ON or independent thereof—is an essential characteristic in rating the usefulness of OCT as a potential marker of axonal loss in longitudinal clinical trials. For MS-ON eyes it has previously been shown that RNFL thinning occurs within the first 6 months after the ON attack [21, 50]. Overall little is known about temporal dynamics of retinal thinning in MS-NON eyes. Based on published data from cross-sectional studies in MS patients with different disease duration a rough estimate of the yearly atrophy rate appears to be around 1 μm/year, which is ten times as much as what can be expected from normal ageing [3]. In previous cross-sectional studies significant inverse correlations of RNFL thickness and disease duration could be established by some authors [11, 15, 24], while others did not find a significant correlation [20, 31]. In PPMS, an MS subtype in which frequency of clinical attacks of ON is probably lowest, Henderson et al. [31] estimated an RNFL thinning of approximately 0.12 μm (TMV reduction: 0.01 mm^3) per year of disease, which is in good agreement with our results in PPMS eyes (RNFL thinning -0.105 μm/year; TMV reduction: -0.011 mm^3/year). Correlations of OCT measures of retinal atrophy and disease duration were not significant for PPMS patients in both studies. In case of RRMS and SPMS patients without ON we estimated higher yearly RNFL changes than for PPMS (nearly 0.5 μm/year). It is, however, important to note that yearly atrophy rates are considerably lower than the optimized axial resolution of SD-OCT devices, which is approximately 4–6 μm [51, 52]. This is of relevance in case OCT endpoints are taken into consideration for future clinical trials, for example, in proof-of-concept trials for neuroprotective agents. Depending on the disease subtypes, model timelines and sample sizes have to be planned accordingly.

In a first longitudinal OCT study by Talman et al. [53] a thorough examination of the time course of RNFL thinning in a mixed cohort of different MS subtypes was performed with TD-OCT (Stratus) revealing a yearly loss of approximately 2 μm in MS-NON eyes (GEE: $P < 0.001$). The study included a preliminary sample size calculation (supplementary data of [53]) for future clinical trials that aimed to detect a 30% reduction in the proportion of eyes with an RNFL

thinning greater than the test-retest variability of the Stratus OCT (6.6 μm) over a follow-up period of 2-3 years. With a power of 80–90% and a type 1 error of 0.05, the authors' sample size calculation estimated roughly a number of 400–600 patients per group. The yearly loss of 2 μm reported by Talman et al. from Stratus OCT is considerably higher than the yearly reduction of approximately 0.5 μm calculated from our dataset. Discrepancies may derive from the differences in the devices applied (TD-OCT versus SD-OCT) and the fact that our calculation is based on cross-sectional data only.

In sum, this study, based on a large SD-OCT data set, confirms previous data on neuroaxonal retinal damage in MS subtypes. At the same time, it extends previous findings by providing new insights into differences between MS-ON and MS-NON eyes in the various subgroups and—in addition—allowing for reliable correction for non-disease-related factors such as age, gender disease duration, and severity.

Authors' Contribution

T. Oberwahrenbrock, S. Schippling, and M. Ringelstein contributed equally to this work.

Acknowledgments

This study was supported by DFG Exc Grant 257 and BMWi Grant ZIM KF2286101FO9. The inims is supported by an unrestricted grant of the "Gemeinnützige Hertie-Stiftung".

References

[1] A. Compston and A. Coles, "Multiple sclerosis," *The Lancet*, vol. 372, no. 9648, pp. 1502–1517, 2008.

[2] D. Huang, E. A. Swanson, C. P. Lin et al., "Optical coherence tomography," *Science*, vol. 254, no. 5035, pp. 1178–1181, 1991.

[3] A. Petzold, J. F. de Boer, S. Schippling et al., "Optical coherence tomography in multiple sclerosis: a systematic review and meta-analysis," *The Lancet Neurology*, vol. 9, no. 9, pp. 921–932, 2010.

[4] C. F. Pfueller, A. U. Brandt, F. Schubert et al., "Metabolic changes in the visual cortex are linked to retinal nerve fiber layer thinning in multiple sclerosis," *PLoS One*, vol. 6, no. 4, Article ID e18019, 2011.

[5] J. Dörr, K. D. Wernecke, M. Bock et al., "Association of retinal and macular damage with brain atrophy in multiple sclerosis," *PLoS One*, vol. 6, no. 4, Article ID e18132, 2011.

[6] E. Gordon-Lipkin, B. Chodkowski, D. S. Reich et al., "Retinal nerve fiber layer is associated with brain atrophy in multiple sclerosis," *Neurology*, vol. 69, no. 16, pp. 1603–1609, 2007.

[7] J. Sepulcre, M. Murie-Fernandez, A. Salinas-Alaman, A. García-Layana, B. Bejarano, and P. Villoslada, "Diagnostic accuracy of retinal abnormalities in predicting disease activity in MS," *Neurology*, vol. 68, no. 18, pp. 1488–1494, 2007.

[8] F. Costello, "Evaluating the use of optical coherence tomography in optic neuritis," *Multiple Sclerosis International*, vol. 2011, Article ID 148394, 9 pages, 2011.

[9] E. M. Frohman, M. G. Dwyer, T. Frohman et al., "Relationship of optic nerve and brain conventional and non-conventional MRI measures and retinal nerve fiber layer thickness, as assessed by OCT and GDx: a pilot study," *Journal of the Neurological Sciences*, vol. 282, no. 1-2, pp. 96–105, 2009.

[10] E. Grazioli, R. Zivadinov, B. Weinstock-Guttman et al., "Retinal nerve fiber layer thickness is associated with brain MRI outcomes in multiple sclerosis," *Journal of the Neurological Sciences*, vol. 268, no. 1-2, pp. 12–17, 2008.

[11] M. Siger, K. Dzięgielewski, L. Jasek et al., "Optical coherence tomography in multiple sclerosis: thickness of the retinal nerve fiber layer as a potential measure of axonal loss and brain atrophy," *Journal of Neurology*, vol. 255, no. 10, pp. 1555–1560, 2008.

[12] J. Toledo, J. Sepulcre, A. Salinas-Alaman et al., "Retinal nerve fiber layer atrophy is associated with physical and cognitive disability in multiple sclerosis," *Multiple Sclerosis*, vol. 14, no. 7, pp. 906–912, 2008.

[13] B. M. Burkholder, B. Osborne, M. J. Loguidice et al., "Macular volume determined by optical coherence tomography as a measure of neuronal loss in multiple sclerosis," *Archives of Neurology*, vol. 66, no. 11, pp. 1366–1372, 2009.

[14] M. Bock, A. U. Brandt, J. Kuchenbecker et al., "Impairment of contrast visual acuity as a functional correlate of retinal nerve fibre layer thinning and total macular volume reduction in multiple sclerosis," *British Journal of Ophthalmology*, vol. 96, no. 1, pp. 62–67, 2011.

[15] J. B. Fisher, D. A. Jacobs, C. E. Markowitz et al., "Relation of visual function to retinal nerve fiber layer thickness in multiple sclerosis," *Ophthalmology*, vol. 113, no. 2, pp. 324–332, 2006.

[16] S. Saidha, S. B. Syc, M. K. Durbin et al., "Visual dysfunction in multiple sclerosis correlates better with optical coherence tomography derived estimates of macular ganglion cell layer thickness than peripapillary retinal nerve fiber layer thickness," *Multiple Sclerosis*, vol. 17, no. 12, pp. 1449–1463, 2011.

[17] S. Noval, I. Contreras, S. Muñoz, C. Oreja-Guevara, B. Manzano, and G. Rebolleda, "Optical coherence tomography in multiple sclerosis and neuromyelitis optica: an update," *Multiple Sclerosis International*, vol. 2011, Article ID 472790, 11 pages, 2011.

[18] M. Bock, A. U. Brandt, J. Dörr et al., "Patterns of retinal nerve fiber layer loss in multiple sclerosis patients with or without optic neuritis and glaucoma patients," *Clinical Neurology and Neurosurgery*, vol. 112, no. 8, pp. 647–652, 2010.

[19] F. Costello, S. Coupland, W. Hodge et al., "Quantifying axonal loss after optic neuritis with optical coherence tomography," *Annals of Neurology*, vol. 59, no. 6, pp. 963–969, 2006.

[20] A. Klistorner, H. Arvind, T. Nguyen et al., "Axonal loss and myelin in early on loss in postacute optic neuritis," *Annals of Neurology*, vol. 64, no. 3, pp. 325–331, 2008.

[21] S. A. Trip, P. G. Schlottmann, S. J. Jones et al., "Retinal nerve fiber layer axonal loss and visual dysfunction in optic neuritis," *Annals of Neurology*, vol. 58, no. 3, pp. 383–391, 2005.

[22] S. Saidha, S. B. Syc, M. A. Ibrahim et al., "Primary retinal pathology in multiple sclerosis as detected by optical coherence tomography," *Brain*, vol. 134, no. 2, pp. 518–533, 2011.

[23] A. U. Brandt, T. Oberwahrenbrock, M. Ringelstein et al., "Primary retinal pathology in multiple sclerosis as detected by optical coherence tomography," *Brain*, vol. 134, no. 11, article e193, 2011.

[24] V. Pueyo, J. Martin, J. Fernandez et al., "Axonal loss in the retinal nerve fiber layer in patients with multiple sclerosis," *Multiple Sclerosis*, vol. 14, no. 5, pp. 609–614, 2008.

[25] M. S. Zaveri, A. Conger, A. Salter et al., "Retinal imaging by laser polarimetry and optical coherence tomography evidence of axonal degeneration in multiple sclerosis," *Archives of Neurology*, vol. 65, no. 7, pp. 924–928, 2008.

[26] S. B. Syc, S. Saidha, S. D. Newsome et al., "Optical coherence tomography segmentation reveals ganglion cell layer pathology after optic neuritis," *Brain*, vol. 135, no. 2, pp. 521–533, 2012.

[27] A. P. D. Henderson, D. R. Altmann, S. A. Trip et al., "Early factors associated with axonal loss after optic neuritis," *Annals of Neurology*, vol. 70, no. 6, pp. 955–963, 2011.

[28] E. Garcia-Martin, V. Pueyo, J. R. Ara et al., "Effect of optic neuritis on progressive axonal damage in multiple sclerosis patients," *Multiple Sclerosis*, vol. 17, no. 7, pp. 830–837, 2011.

[29] P. Albrecht, M. Ringelstein, A.-M. Müller et al., "Degeneration of retinal layers in multiple sclerosis subtypes quantified by optical coherence tomography," *Multiple Sclerosis Journal*. In press.

[30] M. Pulicken, E. Gordon-Lipkin, L. J. Balcer, E. Frohman, G. Cutter, and P. A. Calabresi, "Optical coherence tomography and disease subtype in multiple sclerosis," *Neurology*, vol. 69, no. 22, pp. 2085–2092, 2007.

[31] A. P. D. Henderson, S. A. Trip, P. G. Schlottmann et al., "An investigation of the retinal nerve fibre layer in progressive multiple sclerosis using optical coherence tomography," *Brain*, vol. 131, no. 1, pp. 277–287, 2008.

[32] F. Costello, W. Hodge, Y. I. Pan, M. Freedman, and C. DeMeulemeester, "Differences in retinal nerve fiber layer atrophy between multiple sclerosis subtypes," *Journal of the Neurological Sciences*, vol. 281, no. 1-2, pp. 74–79, 2009.

[33] T. A. Siepman, M. W. Bettink-Remeijer, and R. Q. Hintzen, "Retinal nerve fiber layer thickness in subgroups of multiple sclerosis, measured by optical coherence tomography and scanning laser polarimetry," *Journal of neurology*, vol. 257, no. 10, pp. 1654–1660, 2010.

[34] N. Serbecic, F. Aboul-Enein, S. C. Beutelspacher et al., "Heterogeneous pattern of retinal nerve fiber layer in multiple sclerosis. high resolution optical coherence tomography: potential and limitations," *PLoS One*, vol. 5, no. 11, Article ID e13877, 2010.

[35] M. Bock, A. U. Brandt, J. Dörr et al., "Time domain and spectral domain optical coherence tomography in multiple sclerosis: a comparative cross-sectional study," *Multiple Sclerosis*, vol. 16, no. 7, pp. 893–896, 2010.

[36] S. B. Syc, C. V. Warner, G. S. Hiremath et al., "Reproducibility of high-resolution optical coherence tomography in multiple sclerosis," *Multiple Sclerosis*, vol. 16, no. 7, pp. 829–839, 2010.

[37] N. Serbecic, F. Aboul-Enein, S. C. Beutelspacher et al., "High resolution spectral domain optical coherence tomography (SD-OCT) in multiple sclerosis: the first follow up study over two years," *PLoS One*, vol. 6, no. 5, Article ID e19843, 2011.

[38] C. V. Warner, S. B. Syc, A. M. Stankiewicz et al., "The impact of utilizing different optical coherence tomography devices for clinical purposes and in multiple sclerosis trials," *PLoS One*, vol. 6, no. 8, Article ID e22947, 2011.

[39] C. H. Polman, S. C. Reingold, G. Edan et al., "Diagnostic criteria for multiple sclerosis: 2005 Revisions to the 'McDonald Criteria'," *Annals of Neurology*, vol. 58, no. 6, pp. 840–846, 2005.

[40] F. D. Lublin and S. C. Reingold, "Defining the clinical course of multiple sclerosis: results of an international survey," *Neurology*, vol. 46, no. 4, pp. 907–911, 1996.

[41] J. F. Kurtzke, "Rating neurologic impairment in multiple sclerosis: an expanded disability status scale (EDSS)," *Neurology*, vol. 33, no. 11, pp. 1444–1452, 1983.

[42] F. Costello, W. Hodge, Y. I. Pan, E. Eggenberger, and M. S. Freedman, "Using retinal architecture to help characterize multiple sclerosis patients," *Canadian Journal of Ophthalmology*, vol. 45, no. 5, pp. 520–526, 2010.

[43] A. P. D. Henderson, S. A. Trip, P. G. Schlottmann et al., "A preliminary longitudinal study of the retinal nerve fiber layer in progressive multiple sclerosis," *Journal of Neurology*, vol. 257, no. 7, pp. 1083–1091, 2010.

[44] G. V. McDonnell and S. A. Hawkins, "Clinical study of primary progressive multiple sclerosis in Northern Ireland, UK," *Journal of Neurology Neurosurgery and Psychiatry*, vol. 64, no. 4, pp. 451–454, 1998.

[45] U. Rot and A. Mesec, "Clinical, MRI, CSF and electrophysiological findings in different stages of multiple sclerosis," *Clinical Neurology and Neurosurgery*, vol. 108, no. 3, pp. 271–274, 2006.

[46] N. De Stefano, A. Giorgio, M. Battaglini et al., "Assessing brain atrophy rates in a large population of untreated multiple sclerosis subtypes," *Neurology*, vol. 74, no. 23, pp. 1868–1876, 2010.

[47] E. Tátrai, M. Simó, A. Iljicsov, J. Németh, D. C. DeBuc, and G. M. Somfai, "In vivo evaluation of retinal neurodegeneration in patients with multiple sclerosis," *PLoS One*, vol. 7, no. 1, Article ID e30922, 2012.

[48] P. Tewarie, L. Balk, F. Costello et al., "The OSCAR-IB consensus criteria for retinal OCT quality assessment," *PLoS One*, vol. 7, no. 4, Article ID e34823, 2012.

[49] N. Serbecic, S. C. Beutelspacher, F. C. Aboul-Enein, K. Kircher, A. Reitner, and U. Schmidt-Erfurth, "Reproducibility of high-resolution optical coherence tomography measurements of the nerve fibre layer with the new Heidelberg Spectralis optical coherence tomography," *British Journal of Ophthalmology*, vol. 95, no. 6, pp. 804–810, 2011.

[50] F. Costello, W. Hodge, Y. I. Pan, E. Eggenberger, S. Coupland, and R. H. Kardon, "Tracking retinal nerve fiber layer loss after optic neuritis: a prospective study using optical coherence tomography," *Multiple Sclerosis*, vol. 14, no. 7, pp. 893–905, 2008.

[51] U. E. K. Wolf-Schnurrbusch, L. Ceklic, C. K. Brinkmann et al., "Macular thickness measurements in healthy eyes using six different optical coherence tomography instruments," *Investigative Ophthalmology and Visual Science*, vol. 50, no. 7, pp. 3432–3437, 2009.

[52] B. B. Tan, M. Natividad, K.-C. Chua, and L. W. Yip, "Comparison of retinal nerve fiber layer measurement between 2 spectral domain oct instruments," *Journal of Glaucoma*, vol. 21, no. 4, pp. 266–273, 2012.

[53] L. S. Talman, E. R. Bisker, D. J. Sackel et al., "Longitudinal study of vision and retinal nerve fiber layer thickness in multiple sclerosis," *Annals of Neurology*, vol. 67, no. 6, pp. 749–760, 2010.

11. Lebenslauf

Mein Lebenslauf wird aus datenschutzrechtlichen Gründen in der elektronischen Version meiner Arbeit nicht veröffentlicht.

12. Liste eigener Publikationen

12.1. Originalarbeiten

1. **Kaufhold F**, Kadas EM, Schmidt C, Kunte H, Hoffmann J, Zimmermann H, Oberwahrenbrock T, Harms L, Polthier K, Brandt AU, Paul F (2012).
Optic Nerve Head Quantification in Idiopathic Intracranial Hypertension by Spectral Domain OCT. PLoS ONE 7(5): e36965.

2. Brandt AU, Zimmermann H, **Kaufhold F**, Promesberger J, Schippling S, Finis D, Aktas O, Geis C, Ringelstein M, Ringelstein EB, Hartung HP, Paul F, Kleffner I, Dörr J (2012).
Patterns of Retinal Damage Facilitate Differential Diagnosis between Susac Syndrome and MS. PLoS ONE 7(6): e38741

3. Oberwahrenbrock T, Schippling S, Ringelstein M, **Kaufhold F**, Zimmermann H, Keser N, Young KL, Harmel J, Hartung HP, Martin R, Paul F, Aktas O, Brandt AU (2012).
Retinal Damage in Multiple Sclerosis Disease Subtypes Measured by High-Resolution Optical Coherence Tomography. Multiple Sclerosis International. 2012;2012:1–10.

4. Zimmermann H, Freing A, **Kaufhold F**, Gaede G, Bohn E, Bock M, Oberwahrenbrock T, Young KL, Dörr J, Würfel J, Schippling S, Paul F, Brandt AU (2012).
Optic neuritis interferes with optical coherence tomography and magnetic resonance imaging correlations. Mult. Scler. 2012 Aug 30.

5. Schneider E, Zimmermann H, Oberwahrenbrock T, **Kaufhold F**, Kadas EM, Petzold A, Bilger F, Borisow N, Jarius S, Wildemann B, Ruprecht K, Brandt AU, Paul F (2013).
Optical Coherence Tomography Reveals Distinct Patterns of Retinal Damage in Neuromyelitis Optica and Multiple Sclerosis. PLoS ONE 8(6): e66151.

6. **Kaufhold F**, Zimmermann H, Schneider E, Ruprecht K, Paul F, Oberwahrenbrock T, Brandt AU (2013).

Optic Neuritis Is Associated with Inner Nuclear Layer Thickening and Microcystic Macular Edema Independently of Multiple Sclerosis. PLoS ONE 8(8): e71145.

12.2. Kongressbeiträge

2011

Pattern of retinal alteration in different types of multiple sclerosis measured by high-resolution optical coherence tomography
Oberwahrenbrock T, Ringelstein M, Young KL, **Kaufhold F**, Zimmermann H, Keser N, Hartung HP, Martin R, Aktas O, Schippling S, Paul F, Brandt AU
5TH Joint Trinneal Congress of the European and Americas Committees for Treatment and Research in Multiple Sclerosis, 19 – 22 October 2011, Amsterdam, The Netherlands.
Oral presentations. Mult Scler. 2011 Okt 1;17(10 suppl):S9–S52.

Association of retinal nerve fibre layer and optic nerve head in spectral-domain optical coherence tomography with brain atrophy in multiple sclerosis
Zimmermann HG, Freing A, Oberwahrenbrock T, Gaede G, **Kaufhold F**, Schippling S, Wuerfel JT, Brandt AU, Paul F
5TH Joint Trinneal Congress of the European and Americas Committees for Treatment and Research in Multiple Sclerosis, 19 – 22 October 2011, Amsterdam, NL

2012

3D Optic Nerve Head Segmentation in Idiopathic Intracranial Hypertension
Kadas EM, **Kaufhold F**, Schulz C, Paul F, Polthier K, Brandt AU
In: Tolxdorff T, Deserno TM, Handels H, Meinzer H-P, Herausgeber. Bildverarbeitung für die Medizin 2012 [Internet]. Springer Berlin Heidelberg; 2012 [zitiert 2012 Aug 7]. p. 262–7. Available von:
http://www.springerlink.com/content/p551004423q6131w/abstract/

Association of retinal nerve fibre and ganglion cell layer measures with grey- and white-matter atrophy in multiple sclerosis
Zimmermann H, Freing A, Oberwahrenbrock T, Gaede G, **Kaufhold F**, Schippling S, Wuerfel J, Doerr J, Paul F, Brandt AU
Twenty-second Meeting of the European Neurological Society, 9 – 12 June 2012, Prague, Czech Republic

Characterising neuronal damage in multiple sclerosis using optic nerve head volume
Zimmermann H, Kadas EM, Freing A, **Kaufhold F**, Paul F, Brandt AU
28TH Congress of the European Committee for Treatment and Research in Multiple Sclerosis, 10 - 13 October 2012, Lyon, France

2013

Microcystic macular edema is associated with optic neuritis independently of multiple sclerosis
Kaufhold F, Zimmermann H, Schneider E, Paul F, Oberwahrenbrock T, Brandt AU
65TH Annual meeting of the American Academy of Neurology, 16 – 23 March 2013, San Diego, USA

13. Danksagung

An dieser Stelle möchte ich mich bei allen Mitarbeitern der Arbeitsgruppe klinische Neuroimmunologie des NCRC, sowie Mitarbeitern des DIAL-Teams, die mir stets hilfreich zur Seite standen und versuchten alle meine Fragen und Probleme schnellstmöglich zu klären, bedanken. Mein besonderer Dank gilt in diesem Zusammenhang Herrn Alexander Brandt und Herrn Timm Oberwahrenbrock für die intensive Zusammenarbeit und Förderung der Publikationen im Rahmen dieser Dissertation. Ihre Unterstützung ermöglichte es mir die Anforderungen unserer wissenschaftlichen Projekte schnell und zielstrebig zu bewältigen.

Mein besonderer Dank gilt Herrn Prof. Dr. med. Friedemann Paul für sein Vertrauen in mich, die Förderung meiner wissenschaftlichen Talente und die umfangreiche Betreuung dieser Dissertation. Er ermutigte mich stets unsere Projekte aus einem anderen Blickwinkel zu betrachten und somit meine Fähigkeiten und wissenschaftlichen Erkenntnisse vielseitig weiterzuentwickeln.